

# Entangling distant systems via universal nonadiabatic passage

Zhu-yao Jin<sup>1</sup> and Jun Jing<sup>1,\*</sup>

<sup>1</sup>*School of Physics, Zhejiang University, Hangzhou 310027, Zhejiang, China*

(Dated: November 1, 2024)

In this work, we derive universal nonadiabatic passages in an  $M + N$ -dimensional discrete system, where  $M$  and  $N$  denote the degrees of freedom for the assistant and working subspaces, respectively, that could be separated due to rotation or energy. A systematic method is provided to construct parametric ancillary bases for the nonadiabatic passages, which can set up connection between arbitrary initial and target states. In applications, a transitionless dynamics determined by the von Neumann equation with the time-dependent system Hamiltonian can be formulated to entangle distant qubits, as a vital prerequisite for the practical quantum networks. Using tunable longitudinal interaction between two distant qubits, the superconducting system evolves to the single-excitation Bell state with a fidelity as high as  $F = 0.997$  from the ground state. When the longitudinal interaction is switched off, the single-excitation Bell state can be further converted to the double-excitation Bell state with  $F = 0.982$  by parametric driving. Moreover, our protocol can be adapted to generate the Greenberger-Horne-Zeilinger state for  $N$  qubits with  $N$  steps. Our work develops a full-fledged theory for nonadiabatic state engineering in quantum information processing, which is flexible in target selection and robust against the external noise.

## I. INTRODUCTION

Quantum entanglement [1–3] is an essential resource [4] for quantum information processing [5–9]. Remote entangled systems are desired for many quantum communication protocols, including quantum teleportation [10], quantum key distribution [11, 12], quantum secret sharing [13], quantum secure communication [14], and quantum repeaters [15]. Bell states [16] are the most popular states with maximal entanglement. They can be categorized into the single-excitation and double-excitation entangled states, i.e.,  $|\psi_{\pm}\rangle = (|eg\rangle \pm |ge\rangle)/\sqrt{2}$  and  $|\varphi_{\pm}\rangle = (|ee\rangle \pm |gg\rangle)/\sqrt{2}$ , where  $|e\rangle$  and  $|g\rangle$  denote the excited and ground states of the two-state system, respectively. More generally, the maximally entangled states for  $N$  particles include the Greenberger-Horne-Zeilinger (GHZ) states [17, 18], i.e.,  $(|e\rangle^{\otimes N} + |g\rangle^{\otimes N})/\sqrt{2}$  and the Werner state [19, 20], i.e.,  $(|egg\cdots g\rangle + |geg\cdots g\rangle + \cdots + |ggg\cdots e\rangle)/\sqrt{N}$ . While the latter is more robust against the external noise [16] than the former; the former has a dramatic application in high-precision metrology [21, 22].

Creating the maximal entanglement between neighboring two-state systems has been proposed and realized in various platforms, including cavity QED systems [23, 24], hybrid cavity-magnon systems [25, 26], superconducting circuits [27, 28], and neutral cold atoms [29]. As a key element for quantum network [30–32], long-range entanglement has been proposed in a superconducting waveguide QED system [33]. It remains, however, a challenge to effectively engineer a high-fidelity entanglement for far-away qubits due to the rapid-decaying coupling strength with distance. Recently, the so-called Andreev spin qubit (ASQ) [34–41], i.e., the semiconducting spin qubit embedded into a Josephson junction [42, 43], has attracted

considerable attention due to their long lifetime ( $\sim 20\mu\text{s}$ ) and small size ( $\sim 100\text{nm}$  [44]), which is interested to the large-scale quantum devices. More than the strong exchange coupling between ASQs and superconducting circuits [34, 35], a strong, long-range, and tunable longitudinal interaction among ASQs [41] has been experimentally established by the spin-dependent supercurrent [34–40]. It could become a promising platform for generation and conversion of the maximally entangled states of distant qubits.

Quantum state engineering is primarily motivated to steer the system from a fiducial state to a predetermined target state. Adiabatic protocols, such as stimulated Raman adiabatic passage [45, 46], have found wide-range applications due to its simplicity and robustness against systematic errors. However, the long evolution time of the open quantum systems [47] will lead to the inconvenient decoherence effect on the engineering protocols for such as generation of the entangled states [48, 49]. Various nonadiabatic methods have been proposed to accelerate the passage, such as the holonomic quantum transformation [50–52] and the shortcut to adiabaticity [46, 53–59]. The latter includes the Lewis-Riesenfeld theory for invariant [56, 57] and the counterdiabatic driving method in the adiabatic [53] and dressed-state bases [54, 55]. They can be unified by a perspective on nonadiabatic quantum control [60]. In particular, any nonadiabatic control can be performed along the instantaneous bases in the ancillary picture, which satisfy the von Neumann equation with the time-dependent system Hamiltonian. Despite the versatility of this universal theory, it lacks a systematic way to explicitly formulate the ancillary bases for a discrete system of any size and the application in multi-particle systems.

Using the von Neumann equation for the ancillary bases, this paper presents the relation between the degrees of freedom of the time-dependent Hamiltonian and the nonadiabatic passages and proposes to generate and

---

\* Email address: jingjun@zju.edu.cn

convert entangled states of distant qubits with a high fidelity. We separate the full Hilbert space of a general discrete system of a finite size into the working subspace and the assistant subspace, which can be separated but not limited to the energy splitting. In addition to find the nonadiabatic passages across the two subspaces for fast engineering over system state, we can determine the condition for converting static dark states to useful passages. Then we apply the theoretical framework to generate distant entanglement in a superconducting system that two distant ASQs are indirectly coupled with a strong and tunable longitudinal interaction [41]. Our protocol is superior to the existence in a superconducting waveguide QED system [33] with respect to the fidelity and the range of the target entangled states. We can faithfully realize the mutual conversion between single-excitation and double-excitation Bell states. Moreover, our protocol can generate GHZ states for  $N$  qubits in  $N$  steps. Each step is characterized with fixed control qubits and driving pulses.

The rest part of this paper is structured as follows. In Sec. II A, we briefly review the theory of nonadiabatic control in which the transitionless dynamics is running in the ancillary picture. In Sec. II B, we formulate the ancillary bases for a general  $M + N$ -level system, and find a sufficient condition for converting the dark states to the nonadiabatic passages. In Sec. II C, the  $1 + N$  and  $2 + N$  systems are exemplified to further illustrate our full-fledged nonadiabatic control theory. Section III contributes to generating high-fidelity entangled states of distant Andreev spin qubits in superconducting systems, including Bell states and multi-particle GHZ state. We also demonstrate the conversion between different types of the Bell states. The whole paper is concluded in Sec. IV. In Appendix A, an iterative recipe is introduced to construct the ancillary bases for an arbitrary discrete time-dependent system.

## II. GENERAL FRAMEWORK

### A. Nonadiabatic control theory

Consider a closed quantum system of arbitrary  $K$  dimensions, driven by a time-dependent Hamiltonian  $H(t)$ . The system dynamics can be described by the time-dependent Schrödinger equation ( $\hbar \equiv 1$ )

$$i \frac{d|\psi_m(t)\rangle}{dt} = H(t)|\psi_m(t)\rangle, \quad (1)$$

where  $|\psi_m(t)\rangle$ 's are the pure-state solutions that constitute a completed set for the system space. Alternatively, the system dynamics could be described in an instantaneous picture with the orthonormal bases  $|\mu_k(t)\rangle$ , which span the same Hilbert space as  $|\psi_m(t)\rangle$ . Distinguished from  $|\psi_m(t)\rangle$ ,  $|\mu_k(t)\rangle$  can be formally determined with no knowledge of the system Hamiltonian  $H(t)$ . A typical set of ancillary bases  $|\mu_k(t)\rangle$  is shown in Eqs. (10), (11),

and (12) and an iterative recipe for constructing the ancillary bases can be found in Appendix A. The unitary transformation linking the solution picture  $|\psi_m(t)\rangle$  and the ancillary picture  $|\mu_k(t)\rangle$  is shown in

$$|\psi_m(t)\rangle = \sum_{k=1}^K c_{mk}(t) |\mu_k(t)\rangle, \quad (2)$$

where  $c_{mk}(t)$  is the element of a  $K \times K$  transformation matrix  $\mathcal{C}$  at the  $m$ th row and the  $k$ th column. Substituting Eq. (2) into Eq. (1), we have  $K^2$  differential equations in all for the matrix elements [51, 60], i.e.,

$$\frac{d}{dt} c_{mk}(t) = i \sum_{n=1}^K [\mathcal{G}_{kn}(t) - \mathcal{D}_{kn}(t)] c_{mn}(t), \quad (3)$$

where  $\mathcal{G}_{kn}(t) \equiv i \langle \mu_k(t) | \dot{\mu}_n(t) \rangle$  and  $\mathcal{D}_{kn}(t) \equiv \langle \mu_k(t) | H(t) | \mu_n(t) \rangle$  represent the geometric and dynamical parts of the proportional factor, respectively. Since each  $c_{mk}(t)$  is coupled to the other  $K - 1$  elements  $c_{mn}(t)$ ,  $1 \leq n \neq k \leq K$ , it is hardly to directly solve Eq. (3).

Dealing with the system Hamiltonian in a time-independent ancillary picture  $|\mu_k(0)\rangle$  is useful to simplify and then at least partially solve Eq. (3). Under the unitary rotation by  $V(t) \equiv \sum_{k=1}^K |\mu_k(t)\rangle \langle \mu_k(0)|$ , we have

$$\begin{aligned} H_{\text{rot}}(t) &= V^\dagger(t) H(t) V(t) - i V^\dagger(t) \frac{d}{dt} V(t) \\ &= - \sum_{k=1}^N \sum_{n=1}^N [\mathcal{G}_{kn}(t) - \mathcal{D}_{kn}(t)] |\mu_k(0)\rangle \langle \mu_n(0)|. \end{aligned} \quad (4)$$

If  $H_{\text{rot}}(t)$  could be diagonalized in the ancillary bases with certain  $k$ 's,  $\{k\} \in \{1, 2, \dots, K\}$ , then the proportional factor  $\mathcal{G}_{kn}(t) - \mathcal{D}_{kn}(t)$  in Eq. (3) becomes vanishing unless  $n = k$  and vice versa. The diagonalization under  $V(t)$  could be full or partial, which is implicitly subject to the degrees of freedom of the system Hamiltonian  $H(t)$ . Practically, we have proved [60] a sufficient and necessary condition that if the projection operator  $\Pi_k(t) \equiv |\mu_k(t)\rangle \langle \mu_k(t)|$  satisfies the von Neumann equation [60]

$$\frac{d}{dt} \Pi_k(t) = -i [H(t), \Pi_k(t)], \quad (5)$$

then  $H_{\text{rot}}(t)$  is diagonalized in the base  $|\mu_k(0)\rangle$  with a non-vanishing diagonal element.

For eligible  $k$ 's, Eq. (3) can be reduced to

$$\frac{d}{dt} c_{mk}(t) = i [\mathcal{G}_{kk}(t) - \mathcal{D}_{kk}(t)] c_{mk}(t). \quad (6)$$

One can immediately find the solution:

$$\begin{aligned} c_{mk}(t) &= e^{i f_k(t)} c_{mk}(0), \\ f_k(t) &\equiv \int_0^t [\mathcal{G}_{kk}(t') - \mathcal{D}_{kk}(t')] dt'. \end{aligned} \quad (7)$$

When  $\{k\} = \{1, 2, \dots, K\}$ ,  $H_{\text{rot}}(t)$  is fully diagonalized, i.e., all the ancillary bases can satisfy the von Neumann equation (5) under a common parametric setting. Consequently, Eqs. (1), (3), and (4) give rise to a full-rank nonadiabatic evolution operator for the system:

$$U(t, 0) = \sum_{k=1}^K e^{if_k(t)} |\mu_k(t)\rangle \langle \mu_k(0)| \quad (8)$$

with the generated phase  $f_k(t)$  in Eq. (7). In this ideal case, the system can be steered along arbitrary one of the ancillary bases,  $|\mu_k(0)\rangle \rightarrow |\mu_k(t)\rangle$ , with no transition among them during the whole evolution.

A trivial solution to the von Neumann equation (5) is the time-independent dark state, i.e.,  $|\mu_k(t)\rangle \Rightarrow |\mu_k\rangle$ , leading to a null result on both sides of Eq. (5) due to  $H(t)|\mu_k\rangle = 0$ . If  $|\mu_k(t)\rangle$  are empowered with a slowly-varying (adiabatic) time-dependence, i.e.,  $d\Pi_k(t)/dt \approx 0$ , these seemingly useless states support the stimulated Raman adiabatic passage [45, 46], that could be regarded as an approximate solution to Eq. (5). In Eq. (4), the non-trivial ancillary bases  $|\mu_k(t)\rangle$  and the to-be-diagonalized Hamiltonian  $H_{\text{rot}}$  are mutually dependent on each other. The implicit connection between the system Hamiltonian  $H(t)$  and  $|\mu_k(t)\rangle$  in the von Neumann equation (5) remains obscure until the ancillary bases are explicitly determined. Then we are motivated to provide a symmetric formulation about the completed and orthonormal ancillary bases.

## B. General two-subspace system

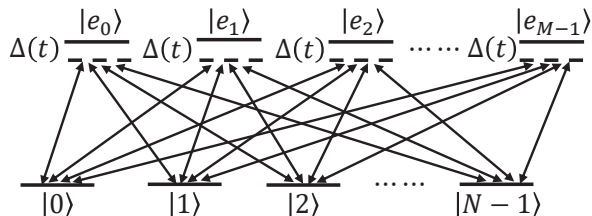


FIG. 1. Sketch of a general  $M + N$ -dimensional system under control. The transition  $|n\rangle \leftrightarrow |e_m\rangle$ ,  $0 \leq n \leq N - 1$  and  $0 \leq m \leq M - 1$ , is driven by the field with the Rabi frequency  $\Omega_n^{(m)}(t)$  and the time-dependent phase  $\varphi_n^{(m)}(t)$ . The upper (assistant) and down (working) subspaces are splitted with the detuning  $\Delta(t)$  in the rotating frame.

We formulate  $|\mu_k(t)\rangle$  in an arbitrary discrete model of  $M + N$  levels, where  $M$  and  $N$  respectively denote the degrees of freedom for the assistant and working subspaces as shown in Fig. 1. Despite this model is treated in a degenerate situation (it is merely for finding compact expressions and yet does not lose generality of our theory), it is still a generalization for the three-level system [45, 46, 50, 51, 53–57, 59], the four-level tripod model [45, 52], and certain multi-level system [45]. These pedagogical models are popular in the

stimulated Raman adiabatic passage [45, 46], the shortcut to adiabaticity [46, 53–59], the adiabatic geometric gates [61, 62], and the nonadiabatic holonomic quantum transformation [50–52]. This model contains all the necessary aspects of the problem at hand and sets our findings on a clear motivation.

We focus on the state engineering based on the driving across the assistant subspace and the working subspace. In particular, the transition between the upper level  $|e_m\rangle$ ,  $m = 0, 1, \dots, M - 1$ , and the down level  $|n\rangle$ ,  $n = 0, 1, \dots, N - 1$ , is induced by the driving field with the time-dependent Rabi-frequency  $\Omega_n^{(m)}(t)$ , phase  $\varphi_n^{(m)}(t)$ , and detuning  $\Delta(t)$ . Then the full Hamiltonian can be written as

$$H(t) = \Delta(t) \sum_{m=0}^{M-1} |e_m\rangle \langle e_m| + \sum_{m=0}^{M-1} \sum_{n=0}^{N-1} \Omega_n^{(m)}(t) e^{i\varphi_n^{(m)}(t)} |e_m\rangle \langle n| + \text{H.c.} \quad (9)$$

It is clearly not the most general configuration due to the lack of the internal driving fields in both subspaces and then it cannot afford a full-rank nonadiabatic control over the whole system. Nevertheless, it is sufficient to have at least two accelerated paths for state transfer across the two subspaces as long as all  $\Omega_n^{(m)}(t)$  are nonvanishing and tunable in time.

In the theoretical framework for nonadiabatic control (see Sec. II A), the system dynamics can be faithfully described in an  $M + N$ -dimensional ancillary picture. Using the iterative recipe in Appendix A, one can formulate a completed and orthonormal set of ancillary bases. In the assistant subspace, we have

$$\begin{aligned} |\tilde{\mu}_0(t)\rangle &= \sin \tilde{\theta}_0(t) |e_0\rangle + \cos \tilde{\theta}_0(t) e^{-i\tilde{\alpha}_0(t)} |e_1\rangle, \\ |\tilde{\mu}_1(t)\rangle &= \sin \tilde{\theta}_1(t) |\tilde{b}_0(t)\rangle + \cos \tilde{\theta}_1(t) e^{-i\tilde{\alpha}_1(t)} |e_2\rangle, \\ &\dots \\ |\tilde{\mu}_{M-2}(t)\rangle &= \sin \tilde{\theta}_{M-2}(t) |\tilde{b}_{M-3}(t)\rangle \\ &\quad + \cos \tilde{\theta}_{M-2}(t) e^{-i\tilde{\alpha}_{M-2}(t)} |e_{M-1}\rangle. \end{aligned} \quad (10)$$

In the working subspace, we have

$$\begin{aligned} |\mu_0(t)\rangle &= \cos \theta_0(t) |0\rangle - \sin \theta_0(t) e^{-i\alpha_0(t)} |1\rangle, \\ |\mu_1(t)\rangle &= \cos \theta_1(t) |b_0(t)\rangle - \sin \theta_1(t) e^{-i\alpha_1(t)} |2\rangle, \\ &\dots \\ |\mu_{N-2}(t)\rangle &= \cos \theta_{N-2}(t) |b_{N-3}(t)\rangle \\ &\quad - \sin \theta_{N-2}(t) e^{-i\alpha_{N-2}(t)} |N-1\rangle. \end{aligned} \quad (11)$$

And the rest bases are across the two subspaces:

$$\begin{aligned} |\mu_{N-1}(t)\rangle &= \cos \phi(t) |b_{N-2}(t)\rangle \\ &\quad - \sin \phi(t) e^{-i\alpha(t)} |\tilde{b}_{M-2}(t)\rangle, \\ |\mu_N(t)\rangle &= \sin \phi(t) |b_{N-2}(t)\rangle + \cos \phi(t) e^{-i\alpha(t)} |\tilde{b}_{M-2}(t)\rangle. \end{aligned} \quad (12)$$

Here the undermined parameters  $\tilde{\theta}_m(t)$ ,  $\theta_n(t)$ , and  $\phi(t)$  are in charge of the population transfer along the nonadiabatic passage;  $\tilde{\alpha}_m(t)$ ,  $\alpha_n(t)$ , and  $\alpha(t)$  control the relative phase among the discrete states; and the  $M + N - 2$  bright states are defined as

$$\begin{aligned}
|\tilde{b}_0(t)\rangle &\equiv \cos \tilde{\theta}_0(t)|e_0\rangle - \sin \tilde{\theta}_0(t)e^{-i\tilde{\alpha}_0(t)}|e_1\rangle, \\
|\tilde{b}_1(t)\rangle &\equiv \cos \tilde{\theta}_1(t)|\tilde{b}_0(t)\rangle - \sin \tilde{\theta}_1(t)e^{-i\tilde{\alpha}_1(t)}|e_2\rangle, \\
&\dots \\
|\tilde{b}_{M-2}(t)\rangle &\equiv \cos \tilde{\theta}_{M-2}(t)|\tilde{b}_{M-3}(t)\rangle \\
&\quad - \sin \tilde{\theta}_{M-2}(t)e^{-i\tilde{\alpha}_{M-2}(t)}|e_{M-1}\rangle, \\
|b_0(t)\rangle &\equiv \sin \theta_0(t)|0\rangle + \cos \theta_0(t)e^{-i\alpha_0(t)}|1\rangle, \\
|b_1(t)\rangle &\equiv \sin \theta_1(t)|b_0(t)\rangle + \cos \theta_1(t)e^{-i\alpha_1(t)}|2\rangle, \\
&\dots \\
|b_{N-2}(t)\rangle &\equiv \sin \theta_{N-2}(t)|b_{N-3}(t)\rangle \\
&\quad + \cos \theta_{N-2}(t)e^{-i\alpha_{N-2}(t)}|N-1\rangle.
\end{aligned} \tag{13}$$

In the same subspace, the bright states and the ancillary bases with the same subscript are orthonormal to each other, i.e.,  $\langle \tilde{\mu}_m(t)|\tilde{b}_m(t)\rangle = 0$  and  $\langle \mu_n(t)|b_n(t)\rangle = 0$ .

The two ancillary bases in Eq. (12), that support the nonadiabatic control, also satisfy  $\langle \mu_{N-1}(t)|\mu_N(t)\rangle = 0$ . By substituting them into the von Neumann equation (5) with the Hamiltonian  $H(t)$  in Eq. (9), the phases, the Rabi frequencies, and the detuning are found to be

$$\begin{aligned}
\varphi_n^{(m)}(t) &= \varphi(t) - \tilde{\alpha}_{m-1}(t) + \alpha_{n-1}(t), \\
\Omega_n^{(m)}(t) &= -\Omega(t) \sin \tilde{\theta}_{m-1}(t) \prod_{m'=m}^{M-2} \cos \tilde{\theta}_{m'}(t) \\
&\quad \times \cos \theta_{n-1}(t) \prod_{n'=n}^{N-2} \sin \theta_{n'}(t), \\
\Delta(t) &= \dot{\alpha}(t) - 2\dot{\phi}(t) \cot[\varphi(t) + \alpha(t)] \cos 2\phi(t), \\
\Omega(t) &= -\dot{\phi}(t) / \sin[\varphi(t) + \alpha(t)]
\end{aligned} \tag{14}$$

where  $n$  ( $m$ ) runs from 0 to  $N - 1$  ( $M - 1$ ),  $\tilde{\alpha}_{-1}(t) \equiv 0$ ,  $\alpha_{-1}(t) \equiv 0$ ,  $\sin \tilde{\theta}_{-1}(t) \equiv -1$ , and  $\cos \theta_{-1}(t) \equiv 1$ . Note  $\Omega(t)$  scales the driving intensity and  $\varphi(t)$  is an arbitrary function of time with no singularity.

We then substitute the ancillary bases of Eqs. (10) and (11) into the von Neumann equation (5). Under these conditions of Eq. (14), the relevant parameters have to be time-independent, i.e.,

$$\begin{aligned}
\tilde{\theta}_m(t) &\rightarrow \tilde{\theta}_m, \quad \tilde{\alpha}_m(t) \rightarrow \tilde{\alpha}_m, \quad m = 0, 1, \dots, M-2, \\
\theta_n(t) &\rightarrow \theta_n, \quad \alpha_n(t) \rightarrow \alpha_n, \quad n = 0, 1, \dots, N-2.
\end{aligned} \tag{15}$$

In this case, the ancillary bases in the assistant and working subspaces become static and some of them are even dark states, i.e.,  $|\tilde{\mu}_m(t)\rangle \rightarrow |\tilde{\mu}_m\rangle$ ,  $|\mu_n(t)\rangle \rightarrow |\mu_n\rangle$ ,  $H(t)|\tilde{\mu}_m\rangle = \Delta(t)|\tilde{\mu}_m\rangle$ , and  $H(t)|\mu_n\rangle = 0$ .

These results can be transparently demonstrated in the

evolution operator (8), which are expressed as

$$\begin{aligned}
U(t, 0) &= \sum_{m=0}^{M-2} e^{i\tilde{f}_m(t)} |\tilde{\mu}_m\rangle \langle \tilde{\mu}_m| + \sum_{n=0}^{N-2} e^{if_n(t)} |\mu_n\rangle \langle \mu_n| \\
&\quad + e^{if_{N-1}(t)} |\mu_{N-1}(t)\rangle \langle \mu_{N-1}(0)| + e^{if_N(t)} |\mu_N(t)\rangle \langle \mu_N(0)|,
\end{aligned} \tag{16}$$

under our Hamiltonian (9). By the definitions in Eq. (7), the generated phases are found to be

$$\begin{aligned}
\tilde{f}_m(t) &= \int_0^t [\tilde{\mathcal{G}}_{mm}(t') - \tilde{\mathcal{D}}_{mm}(t')] dt', \\
f_n(t) &= 0, \quad n \leq M-2 \\
f_{N-1}(t) &= \int_0^t [\mathcal{G}_{N-1, N-1}(t') - \mathcal{D}_{N-1, N-1}(t')] dt, \\
f_N(t) &= \int_0^t [\dot{\alpha}(t') - \Delta(t')] dt' - f_{N-1}(t),
\end{aligned} \tag{17}$$

where  $\tilde{\mathcal{G}}_{mm}(t') = 0$ ,  $\tilde{\mathcal{D}}_{mm}(t') = \Delta(t')$ ,  $\mathcal{G}_{N-1, N-1}(t') = \dot{\alpha}(t) \sin^2 \phi(t)$ , and  $\mathcal{D}_{N-1, N-1}(t') = \Delta(t) \sin^2 \phi(t) - \Omega(t) \sin 2\phi(t) \cos[\varphi(t) + \alpha(t)]$ . Thus the ancillary bases in the assistant subspace  $|\tilde{\mu}_m\rangle$  might gain a global phase  $\tilde{f}_m(t)$  that is purely dynamical; and those in the working subspace  $|\mu_n\rangle$  are completely static. In contrast to these trivial passages, the ancillary bases  $|\mu_{N-1}(t)\rangle$  and  $|\mu_N(t)\rangle$  can be used to transfer population and accumulate the relative phase among desired levels.

Alternatively, the nonadiabatic passage could be observed through the system Hamiltonian  $H(t)$  expanded with the ancillary bases in Eqs. (10), (11), and (12) and the bright states in Eq. (13). Under the conditions in Eqs. (14) and (15), we have

$$\begin{aligned}
H(t) &= \Delta(t) \left[ \sum_{m=0}^{M-2} |\tilde{\mu}_m\rangle \langle \tilde{\mu}_m| + |\tilde{b}_{M-2}\rangle \langle \tilde{b}_{M-2}| \right] \\
&\quad + \Omega(t) e^{i\varphi(t)} |\tilde{b}_{M-2}\rangle \langle b_{N-2}| + \text{H.c.}
\end{aligned} \tag{18}$$

The first line of Eq. (18) contributes to the dynamical phase  $\tilde{f}_m(t)$  on the passage  $|\tilde{\mu}_m\rangle$  in Eq. (16). The second line explains the Rabi oscillation between  $|\mu_{N-1}(t)\rangle$  and  $|\mu_N(t)\rangle$  in Eq. (12), which is the sufficient condition for constructing the nonadiabatic passages along  $|\mu_{N-1}(t)\rangle$  or  $|\mu_N(t)\rangle$  by the von Neumann equation (5).

In addition to them, it is found that any  $|\tilde{\mu}_m\rangle$ ,  $m \in \{0, 1, \dots, M-2\}$ , could be converted to a full-featured state-transfer path with the additional driving fields inside the assistant subspace. For example, consider the full Hamiltonian as

$$\begin{aligned}
H'(t) &= H(t) + h(t), \\
h(t) &= \delta(t) |e_{m+1}\rangle \langle e_{m+1}| \\
&\quad + \sum_{n=0}^m \omega_n^{(m+1)}(t) e^{i\Phi_n^{(m+1)}(t)} |e_{m+1}\rangle \langle e_n| + \text{H.c.},
\end{aligned} \tag{19}$$

where  $\delta(t)$  is the extra detuning for the level  $|e_{m+1}\rangle$ ,  $\omega_n^{(m+1)}(t)$  is the Rabi frequency of the transition

$|e_{m+1}\rangle \leftrightarrow |e_n\rangle$ , and  $\Phi_n^{(m+1)}(t)$  is a time-dependent phase. Substituting the ancillary base  $|\tilde{\mu}_m(t)\rangle$  of Eq. (10) and the ancillary bases  $|\mu_{N-1}(t)\rangle$  and  $|\mu_N(t)\rangle$  of Eq. (12) into the von Neumann equation (5) with the system Hamiltonian (19), we can obtain

$$\begin{aligned}\Phi_n^{(m+1)}(t) &= \frac{\pi}{2} - \tilde{\alpha}_m(t) + \tilde{\alpha}_{n-1}, \quad 0 \leq n \leq m \\ \omega_n^{(m+1)}(t) &= -\omega(t) \sin \tilde{\theta}_{n-1} \prod_{m'=n}^{m-1} \cos \tilde{\theta}_{m'}, \\ \omega(t) &= -\dot{\theta}_m(t), \\ \delta(t) &= \dot{\tilde{\alpha}}_m(t),\end{aligned}\quad (20)$$

in addition to Eq. (14) and the second line of Eq. (15). Equivalently, we find that the auxiliary system Hamiltonian

$$h(t) = \omega(t) e^{i\pi/2 - i\tilde{\alpha}_m(t)} |e_{m+1}\rangle \langle \tilde{b}_{m-1}(t)| + \text{H.c.} \quad (21)$$

gives rise to the third nonadiabatic passage  $|\tilde{\mu}_m(t)\rangle$ , under the conditions of (14), (15), and (20).

Similarly, if one is desired to convert a dark state  $|\mu_n\rangle$ ,  $n \in \{0, 1, \dots, N-2\}$ , in the working subspace to a nonadiabatic passage, then one has to add an auxiliary system Hamiltonian  $h(t)$  to the original system Hamiltonian (9) as long as  $\langle n+1|h(t)|b_{n-1}\rangle$  is nonvanishing and time-dependent.

### C. Illustrative examples

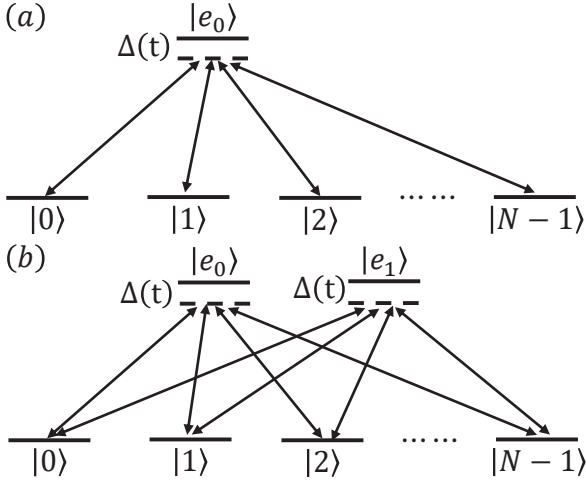


FIG. 2. Sketch of (a)  $1 + N$ -dimensional and (b)  $2 + N$ -dimensional systems under control. The transition  $|n\rangle \leftrightarrow |e_m\rangle$ ,  $0 \leq n \leq N-1$  and  $m = 0, 1$ , is driven by the field with Rabi-frequency  $\Omega_n^{(m)}(t)$  and phase  $\varphi_n^{(m)}(t)$ .

In this subsection, we exemplify the general model in Fig. 1 with the  $1 + N$ -dimensional and  $2 + N$ -dimensional systems as shown in Fig. 2(a) and 2(b), respectively,

to further illustrate the nonadiabatic control theory in Sec. II B. Here the nonadiabatic passages are not beyond the scope of  $|\mu_{N-1}(t)\rangle$  and  $|\mu_N(t)\rangle$ .

For the  $1 + N$ -level system in Fig. 2(a), the transition between  $|e_0\rangle$  and  $|n\rangle$ , where  $n$  runs from 0 to  $N-1$ , is driven by the laser field  $\Omega_n^{(0)}(t)$  with the time-dependent phase  $\varphi_n(t)$  and detuning  $\Delta(t)$ . Then the full Hamiltonian can be written as

$$\begin{aligned}H(t) &= \Delta(t) |e_0\rangle \langle e_0| \\ &+ \left( \sum_{n=0}^{N-1} \Omega_n^{(0)}(t) e^{i\varphi_n^{(0)}(t)} |e_0\rangle \langle n| + \text{H.c.} \right),\end{aligned}\quad (22)$$

It can be reduced from Eq. (9) when the driving field  $\Omega_n^{(m)}$  with  $1 \leq m \leq M-2$  is turned off. In this case, the ancillary bases can be formulated by those for the working subspace, which are exactly the same as Eq. (11), and those involving the working subspace and the upper level  $|e_0\rangle$ :

$$\begin{aligned}|\mu_{N-1}(t)\rangle &= \cos \phi(t) |b_{N-2}(t)\rangle - \sin \phi(t) e^{-i\alpha(t)} |e_0\rangle, \\ |\mu_N(t)\rangle &= \sin \phi(t) |b_{N-2}(t)\rangle + \cos \phi(t) e^{-i\alpha(t)} |e_0\rangle,\end{aligned}\quad (23)$$

where the time-dependent parameter  $\phi(t)$  and the bright state  $|b_{N-2}(t)\rangle$  are the same as those in Eq. (12) and Eq. (13), respectively.

Substituting the ancillary bases  $|\mu_{N-1}(t)\rangle$  and  $|\mu_N(t)\rangle$  in Eq. (23) to the von Neumann equation (5) with the Hamiltonian (22), we have the phases, the Rabi-frequencies, and the detuning as

$$\begin{aligned}\varphi_n^{(0)}(t) &= \varphi(t) + \alpha_{n-1}(t), \quad 0 \leq n \leq N-1, \\ \Omega_n^{(0)}(t) &= \Omega(t) \cos \theta_{n-1}(t) \prod_{n'=n}^{N-1} \sin \theta_{n'}(t), \\ \Delta(t) &= \dot{\alpha}(t) - 2\dot{\phi}(t) \cot[\varphi(t) + \alpha(t)] \cos 2\phi(t).\end{aligned}\quad (24)$$

The time-evolution operator (16) for the full system now becomes

$$\begin{aligned}U(t, 0) &= \sum_{n=0}^{N-2} |\mu_n\rangle \langle \mu_n| + e^{if_{N-1}(t)} |\mu_{N-1}(t)\rangle \langle \mu_{N-1}(0)| \\ &+ e^{if_N(t)} |\mu_N(t)\rangle \langle \mu_N(0)|.\end{aligned}\quad (25)$$

Along the passages  $|\mu_{N-1}(t)\rangle$  and  $|\mu_N(t)\rangle$ , the state transfer and the accumulation of the relative phases can be demonstrated on the discrete states  $|b_{N-2}(t)\rangle$  and  $|e_0\rangle$ .

When  $N = 3$ , the general model in Fig. 2(a) describes a four-level tripod system. It is found that the transformation presented in Eq. (23) and the parametric condition in Eq. (24) can be used to construct the geometric gates in the tripod system [52].

For the  $2 + N$ -dimensional system as shown in Fig. 2(b), the transition between  $|e_m\rangle$  ( $m = 0, 1$ ) and  $|n\rangle$  ( $n = 0, 1, \dots, N-1$ ) is driven by the laser field  $\Omega_n^{(m)}(t)$  with

the time-dependent phase  $\varphi_n^{(m)}(t)$  and the same detuning  $\Delta(t)$ . Then the full Hamiltonian can be written as

$$H(t) = \Delta(t)(|e_0\rangle\langle e_0| + |e_1\rangle\langle e_1|) + \left( \sum_{m=0}^1 \sum_{n=0}^{N-1} \Omega_n^{(m)}(t) e^{i\varphi_n^{(m)}(t)} |e_m\rangle\langle n| + \text{H.c.} \right). \quad (26)$$

In comparison to the case of  $M = 1$  in Fig. 2(a), we now have an ancillary base in the assistant subspace, which is  $|\tilde{\mu}_0(t)\rangle$  in Eq. (10). The ancillary bases  $|\mu_n(t)\rangle$ ,  $n < N - 1$ , for the work subspace remain the same as in Eq. (11). Also the last two bases across two subspaces are the same as Eq. (12) with  $M = 2$ . In this case, the transformation in Eqs. (10), (11), and (12) are equivalent to a general Morris-Shore transformation. When  $N = 3$ , it recovers the result in Ref. [63].

On substituting  $|\mu_{N-1}(t)\rangle$  and  $|\mu_N(t)\rangle$  into the von Neumann equation (5) with the Hamiltonian in Eq. (26), the time-dependent phases, Rabi-frequencies, and detuning are found to satisfy

$$\begin{aligned} \varphi_n^{(0)}(t) &= \varphi(t) + \alpha_{n-1}(t), \quad 0 \leq n \leq N-1, \\ \varphi_n^{(1)}(t) &= \varphi(t) - [\tilde{\alpha}_0(t) - \alpha_{n-1}(t)], \\ \Omega_n^{(0)} &= \Omega(t) \cos \theta_{n-1}(t) \cos \tilde{\theta}_0(t) \prod_{n'=n}^{N-1} \sin \theta_{n'}(t), \\ \Omega_n^{(1)} &= -\Omega(t) \cos \theta_{n-1}(t) \sin \tilde{\theta}_0(t) \prod_{n'=n}^{N-1} \sin \theta_{n'}(t), \\ \Delta(t) &= \dot{\alpha}(t) - 2\dot{\phi}(t) \cot[\varphi(t) + \alpha(t)] \cos 2\phi(t). \end{aligned} \quad (27)$$

They give exactly rise to the nonadiabatic evolution operator (16) with  $M = 2$ .

### III. MAXIMALLY ENTANGLING MULTIPLE DISTANT QUBITS

#### A. Two-qubit system

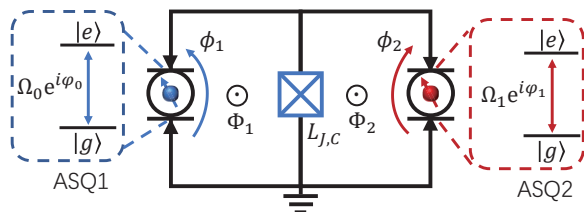


FIG. 3. Sketch of two longitudinally coupled Andreev spin qubits, that connect to a Josephson junction with a tunable Josephson inductance  $L_{J,C}$ . ASQ1 and ASQ2 are respectively driven by the laser fields with the Rabi frequencies  $\Omega_0(t)$  and  $\Omega_1(t)$  and the time-dependent phases  $\varphi_0(t)$  and  $\varphi_1(t)$ .  $\Phi_1$  and  $\Phi_2$  are the magnetic fluxes through the two loops.

Our study of application is conducted in a superconducting system [41] as shown in Fig. 3, which is embed-

ded with two ASQs [34, 35] and a Josephson junction and forms a double-loop superconducting quantum interference device. The full Hamiltonian reads [41],

$$H = \frac{\omega_1}{2} \sigma_1^z + \frac{\omega_2}{2} \sigma_2^z + \frac{J}{2} \sigma_1^z \sigma_2^z, \quad (28)$$

where  $\omega_n$  and  $\sigma_n^z$  denote the transition frequency and the  $Z$  Pauli matrix of the  $n$ th qubit, respectively. For simplicity, we set  $\omega_1 = \omega_2 = \omega$ . The longitudinal interaction between two ASQs can be effectively established via the Josephson junction due to the fact that the spin-dependent supercurrent of ASQ1 induces a spin-dependent flux difference over ASQ2 and then changes its transition frequency by  $J$  [41]. It is tunable by the Josephson inductance  $L_{J,C}$ , the external magnetic field, and the flux through the loop, i.e.,  $\Phi_1$  and  $\Phi_2$ . For the spins separated with a distance of  $\sim 25\mu\text{m}$  [41],  $J/2\pi$  ranges from 0 to 200 MHz.

To generate entanglement in the qubits via the nonadiabatic control in Sec. II, we consider that the ASQ1 and ASQ2 are driven by the laser fields. Then the full Hamiltonian can be written as

$$H_{\text{tot}}(t) = H + H_d(t). \quad (29)$$

Here  $H$  is the original Hamiltonian in Eq. (28) and  $H_d(t)$  is the driving Hamiltonian:

$$H_d(t) = \Omega_0(t) e^{i[\omega_0 t + \varphi_0(t)]} |e\rangle_1 \langle g| + \Omega_1(t) e^{i[\omega_0 t + \varphi_1(t)]} |e\rangle_2 \langle g| + \text{H.c.}, \quad (30)$$

where  $\Omega_0(t)$  and  $\Omega_1(t)$  are Rabi frequencies,  $\omega_0$  is the common driving frequency that is tunable at will, and  $\varphi_0(t)$  and  $\varphi_1(t)$  are the time-dependent phases. In the rotating frame with respect to  $H$  (28), we have

$$\begin{aligned} H_{\text{rot}}(t) &= e^{i(\omega + \omega_0 + J)t} \\ &\times [\Omega_0(t) e^{i\varphi_0(t)} (|ee\rangle \langle ge| + e^{-i2Jt} |eg\rangle \langle gg|) \\ &+ \Omega_1(t) e^{i\varphi_1(t)} (|ee\rangle \langle eg| + e^{-i2Jt} |ge\rangle \langle gg|)] + \text{H.c.} \end{aligned} \quad (31)$$

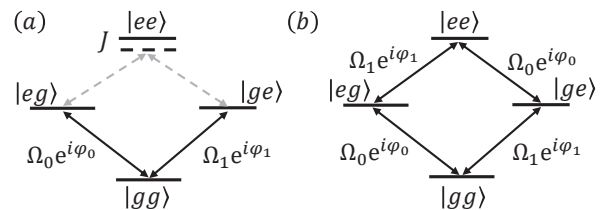


FIG. 4. Transition diagram for the longitudinally coupled two-ASQ system when (a) the driving frequency  $\omega_0 = -\omega + J$  and the coupling strength  $J \gg \{\Omega_0, \Omega_1\}$ , and (b)  $\omega_0 = -\omega$  and  $J = 0$ .

*Step 1*— In this step, we are desired to evolve the system from the ground state  $|gg\rangle$  to the single-excitation Bell state  $(|eg\rangle + |ge\rangle)/\sqrt{2}$ . Using the driving frequency

$\omega_0 = -\omega + J$  and a strong coupling strength  $J \gg \{\Omega_0, \Omega_1\}$ , the Hamiltonian (31) becomes

$$H_{\text{eff}}^{(1)} = \Omega_0(t)e^{i\varphi_0(t)}|eg\rangle\langle gg| + \Omega_1(t)e^{i\varphi_1(t)}|ge\rangle\langle gg| + \text{H.c.} \quad (32)$$

under the rotating-wave approximation. As shown in Fig. 4(a),  $H_{\text{eff}}^{(1)}$  describes a 1+2-dimensional system in the subspace spanned by  $|gg\rangle$ ,  $|eg\rangle$ , and  $|ge\rangle$ , that has been illustrated in Sec. II C. The transitions  $|ee\rangle \leftrightarrow |eg\rangle$  and  $|ee\rangle \leftrightarrow |ge\rangle$  indicated by the gray dashed lines in Fig. 4(a) are suppressed by the strong longitudinal interaction.

As a special case of Eqs. (10), (11), and (12) for  $M = 1$  and  $N = 2$ , the ancillary bases for the working subspace can be chosen as

$$|\mu_0(t)\rangle = \cos\theta_0(t)|eg\rangle - \sin\theta_0(t)e^{-i\alpha_0(t)}|ge\rangle, \quad (33)$$

and those involving the working subspace and the ground level  $|gg\rangle$  are

$$\begin{aligned} |\mu_1(t)\rangle &= \cos\phi(t)|b_0(t)\rangle - \sin\phi(t)e^{-i\alpha(t)}|gg\rangle, \\ |\mu_2(t)\rangle &= \sin\phi(t)|b_0(t)\rangle + \cos\phi(t)e^{-i\alpha(t)}|gg\rangle, \end{aligned} \quad (34)$$

where  $\alpha_0(t)$ ,  $\alpha(t)$ ,  $\theta_0(t)$ , and  $\phi(t)$  are the time-dependent parameters and the bright state is  $|b_0(t)\rangle \equiv \sin\theta_0(t)|eg\rangle + \cos\theta_0(t)e^{-i\alpha_0(t)}|ge\rangle$ .

Substituting  $|\mu_1(t)\rangle$  and  $|\mu_2(t)\rangle$  in Eq. (34) to the von Neumann equation (5) with the Hamiltonian (32), we have the phases and the Rabi-frequencies as

$$\begin{aligned} \varphi_0(t) &= \varphi(t), \\ \varphi_1(t) &= \varphi(t) + \alpha_0(t), \\ \Omega_0(t) &= \Omega(t) \cos\theta_0(t), \\ \Omega_1(t) &= -\Omega(t) \sin\theta_0(t), \\ \dot{\alpha}(t) &= -2\dot{\phi}(t) \cot[\varphi(t) + \alpha(t)] \cot 2\phi(t). \end{aligned} \quad (35)$$

$|\mu_0(t)\rangle$  in Eq. (33) is a dark state. Depending on the boundary conditions of the phases  $\alpha(t)$  and  $\phi(t)$ , the system can alternatively evolve along the passages  $|\mu_1(t)\rangle$  or  $|\mu_2(t)\rangle$ . If  $\alpha(t) = \pi$ ,  $\phi(0) = \pi/2$ , and  $\phi(T) = 0$  with  $T$  the period of state transfer, then the system can evolve from the ground state to the bright state  $|b_0(t)\rangle$  along the passage  $|\mu_1(t)\rangle$ . It is found that the population distribution on the states  $|eg\rangle$  and  $|ge\rangle$  of the target state depends on the parameter  $\theta_0(t)$ , that is determined by the ratio of the driving intensities in Eq. (35). In addition, the relative phase  $\alpha_0(t)$  can be tuned by the phase difference between  $\varphi_0(t)$  and  $\varphi_1(t)$  in Eq. (35). With no loss of generality, we set  $\theta_0 = \pi/4$  and  $\alpha_0 = 0$ , and then the system evolves to the single-excitation Bell state, i.e.,  $|gg\rangle \rightarrow (|eg\rangle + |ge\rangle)/\sqrt{2}$ .

*Step 2*— In this step, we target to perform the mutual conversion between the single-excitation Bell state and the double-excitation Bell state, i.e.,  $(|eg\rangle + |ge\rangle)/\sqrt{2} \leftrightarrow (|ee\rangle - |gg\rangle)/\sqrt{2}$ . We turn off the longitudinal interaction, i.e.,  $J = 0$ , and set the driving frequency as  $\omega_0 = -\omega$ . The Hamiltonian (31) then becomes

$$\begin{aligned} H_{\text{eff}}^{(2)} &= \Omega_0(t)e^{i\varphi_0(t)}(|ee\rangle\langle ge| + |eg\rangle\langle gg|) \\ &+ \Omega_1(t)e^{i\varphi_1(t)}(|ee\rangle\langle eg| + |ge\rangle\langle gg|) + \text{H.c.}, \end{aligned} \quad (36)$$

which forms a 2 + 2-dimensional system as shown in Fig. 4(b). In this step, the states  $|ee\rangle$  and  $|gg\rangle$  constitute the assistant subspace and the states  $|eg\rangle$  and  $|ge\rangle$  span the working subspace.

Similar to Eqs. (10), (11), and (12) for  $M = 2$  and  $N = 2$ , the ancillary bases in this case are found to be

$$\begin{aligned} |\tilde{\mu}_0(t)\rangle &= \sin\tilde{\theta}_0(t)|ee\rangle + \cos\tilde{\theta}_0(t)e^{-i\tilde{\alpha}_0(t)}|gg\rangle, \\ |\mu_0(t)\rangle &= \cos\theta_0(t)|eg\rangle - \sin\theta_0(t)e^{-i\alpha_0(t)}|ge\rangle, \\ |\mu_1(t)\rangle &= \cos\phi(t)|b_0(t)\rangle - \sin\phi(t)e^{-i\alpha(t)}|\tilde{b}_0(t)\rangle, \\ |\mu_2(t)\rangle &= \sin\phi(t)|b_0(t)\rangle + \cos\phi(t)e^{-i\alpha(t)}|\tilde{b}_0(t)\rangle, \end{aligned} \quad (37)$$

where  $\tilde{\alpha}_0(t)$ ,  $\alpha_0(t)$ ,  $\alpha(t)$ ,  $\tilde{\theta}_0(t)$ ,  $\theta_0(t)$ , and  $\phi(t)$  are the time-dependent parameters. Due to Eq. (13), the bright states are

$$\begin{aligned} |\tilde{b}_0(t)\rangle &\equiv \cos\tilde{\theta}_0(t)|ee\rangle - \sin\tilde{\theta}_0(t)e^{-i\tilde{\alpha}_0(t)}|gg\rangle, \\ |b_0(t)\rangle &\equiv \sin\theta_0(t)|eg\rangle + \cos\theta_0(t)e^{-i\alpha_0(t)}|ge\rangle. \end{aligned} \quad (38)$$

Substituting the ancillary bases  $|\mu_1(t)\rangle$  and  $|\mu_2(t)\rangle$  of Eq. (37) into Eq. (5) with the effective Hamiltonian (36), we have

$$\begin{aligned} \varphi_0(t) &= \varphi(t) + \tilde{\alpha}_0(t) + \alpha_0(t), \\ \varphi_1(t) &= \varphi(t), \\ \Omega_0(t) &= \Omega(t) \cos\tilde{\theta}_0(t) \cos\theta_0(t), \\ \Omega_1(t) &= \Omega(t) \cos\tilde{\theta}_0(t) \sin\theta_0(t), \\ \dot{\alpha}(t) &= -2\dot{\phi}(t) \cot[\varphi(t) + \alpha(t)] \cot 2\phi(t), \end{aligned} \quad (39)$$

and we find  $\varphi(t) = \pi/2$ ,  $\tilde{\theta}_0(t) = \pi/4$  and  $\theta_0(t) = \pi/4$ . Under the conditions in Eq. (39),  $|\tilde{\mu}_0(t)\rangle$  and  $|\mu_0(t)\rangle$  in Eq. (37) are dark states, while  $|\mu_1(t)\rangle$  and  $|\mu_2(t)\rangle$  can be used as the nonadiabatic passages. When  $\alpha_0(t) = 0$ ,  $\tilde{\alpha}_0(t) = 0$ ,  $\alpha(t) = \pi$ ,  $\phi(T) = 0$ , and  $\phi(2T) = \pi/2$ , the single-excitation Bell state  $(|eg\rangle + |ge\rangle)/\sqrt{2}$  is found to be converted to the double-excitation Bell state  $(|ee\rangle - |gg\rangle)/\sqrt{2}$  via the path  $|\mu_1(t)\rangle$ . Here we assume that Step 2 lasts the same period of  $T$  as Step 1. In addition, by using proper boundary conditions of  $\alpha_0(t)$ ,  $\tilde{\alpha}_0(t)$ ,  $\alpha(t)$  and  $\phi(t)$ , the conversion in Step 2 can be inverted. For example, when  $\alpha_0(t) = 0$ ,  $\tilde{\alpha}_0(t) = 0$ ,  $\alpha(t) = \pi$ ,  $\phi(T) = \pi/2$ , and  $\phi(2T) = 0$ , if the system is prepared as  $(|ee\rangle - |gg\rangle)/\sqrt{2}$  when  $t = T$ , it can be converted to  $(|eg\rangle + |ge\rangle)/\sqrt{2}$  when  $t = 2T$  via the same path  $|\mu_1(t)\rangle$ .

The performance in generation of Bell states can be measured by the population  $P_n(t) \equiv \langle n|\rho(t)|n\rangle$  over the product states  $|n\rangle$ ,  $n = gg, eg, ge, ee$ , and the target-state fidelity  $\mathcal{F}(t) \equiv \langle \psi_{\text{Bell}}|\rho(t)|\psi_{\text{Bell}}\rangle$ , where  $\rho(t)$  is the time-evolved density matrix for the system qubits. Here in Step 1,  $|\psi_{\text{Bell}}\rangle = (|eg\rangle + |ge\rangle)/\sqrt{2}$ ; and in Step 2,  $|\psi_{\text{Bell}}\rangle = (|ee\rangle - |gg\rangle)/\sqrt{2}$ . And we initially choose  $\rho(0) = |\mu_1(0)\rangle\langle\mu_1(0)|$ . In the presence of external dissipation, the dynamics of population and fidelity can be estimated by the master equation [64],

$$\frac{\partial\rho}{\partial t} = -i[H_{\text{tot}}(t), \rho] + \frac{\kappa}{2}\mathcal{L}(\sigma_1^-) + \frac{\kappa}{2}\mathcal{L}(\sigma_2^-). \quad (40)$$

Here  $H_{\text{tot}}(t)$  is the full Hamiltonian in Eq. (29).  $\mathcal{L}(o)$  is the Lindblad superoperator defined as  $\mathcal{L}(o) \equiv 2\omega\rho o^\dagger - o^\dagger o \rho - \rho o^\dagger o$  [65], where  $o = \sigma_1^-$  and  $\sigma_2^-$ .  $\sigma_n^- \equiv |g\rangle_n \langle e|$  describes the dissipation channel of the  $n$ th qubit. The lifetime of the ASQ is typically in the order of  $\sim 20\mu\text{s}$  [34–40]. Then the decay rate  $\kappa/2\pi \sim 10$  kHz. The running time for each step is set in the order of  $T \sim 1\mu\text{s}$  in our numerical simulation.

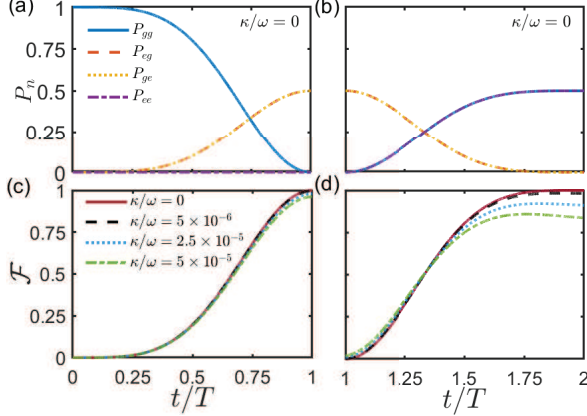


FIG. 5. (a) and (b): Dynamics for the closed system about population  $P_n$ ,  $n = gg, eg, ge, ee$ , during Step 1 and Step 2, respectively. (c) and (d): Target-state fidelity dynamics  $\mathcal{F}$  about the single-excitation Bell state  $(|eg\rangle + |ge\rangle)/\sqrt{2}$  and the double-excitation Bell state  $(|ee\rangle - |gg\rangle)/\sqrt{2}$ , respectively, for both closed and open systems. In (a) and (c),  $\omega_0 = -\omega + J$ ,  $J/\omega = 0.1$ ,  $\theta_0(t) = \pi/4$ ,  $\varphi(t) = \pi/2$ ,  $\alpha_0(t) = 0$ ,  $\alpha(t) = 0$ ,  $\phi(t) = (\pi/2) \cos[\pi t/(2T)]$ , and the Rabi frequencies  $\Omega_n(t)$  and the phases  $\varphi_n(t)$  are set according to Eq. (35). In (b) and (d),  $\omega_0 = -\omega$  and  $J/\omega = 0$ ,  $\varphi(t) = \pi/2$ ,  $\alpha_0(t) = 0$ ,  $\tilde{\alpha}_0(t) = 0$ ,  $\alpha(t) = \pi$ ,  $\phi(t) = (\pi/2) \cos[\pi t/(2T)]$ , and  $\Omega_n(t)$  and  $\varphi_n(t)$  are set according to Eq. (39).

The closed-system dynamics of population are demonstrated in Figs. 5(a) and (b). The effect from external dissipation can be found in the fidelity dynamics in Figs. 5(c) and (d). During the first step  $t \in [0, T]$  as shown in Fig. 5(a), the population on  $|gg\rangle$  is equally transferred to  $|eg\rangle$  and  $|ge\rangle$  and the state  $|ee\rangle$  is never populated as described by  $|\mu_1(t)\rangle$  in Eq. (34). Together with the red solid line in Fig. 5(c), by which a target state  $|\psi_{\text{Bell}}\rangle = (|eg\rangle + |ge\rangle)/\sqrt{2}$  is achieved in the end of Step 1, it confirms that the system described by Fig. 4(a) can be faithfully simplified as a 1+2-dimensional system. In the presence of a dissipative noise, the fidelity at  $t = T$  can be maintained as high as  $F = 0.997$  under the experimentally practical decay rate  $\kappa/\omega = 5 \times 10^{-6}$  [41], by which our protocol prevails over the existing one in the superconducting waveguide QED system [33] with the same target state and the same order of magnitude of noise. Our protocol can tolerate larger decay rates. It is found in Fig. 5(c) that  $F(T) = 0.980$  for  $\kappa/\omega = 2.5 \times 10^{-5}$  and  $F(T) = 0.962$  for  $\kappa/\omega = 5 \times 10^{-5}$ .

During the second step, e.g.,  $t \in [T, 2T]$ , as shown in Fig. 5(b), the states  $|ee\rangle$  and  $|gg\rangle$  are synchronously

populated as the populations on the states  $|eg\rangle$  and  $|ge\rangle$  decrease with time. The relevant dynamics of target-state fidelity for the double-excitation Bell state  $(|ee\rangle - |gg\rangle)/\sqrt{2}$  is shown in Fig. 5(d), which seems more fragile to the dissipative noise than that for the single-excitation Bell state. When  $t = 2T$ , the fidelity can remain almost at unit for  $\kappa/\omega = 5 \times 10^{-6}$ . And it reduces to  $F = 0.912$  for  $\kappa/\omega = 2.5 \times 10^{-5}$  and  $F = 0.836$  for  $\kappa/J = 5 \times 10^{-5}$ .

## B. Three-qubit system

With an extended Hamiltonian as to that in Eq. (29), a GHZ state of 3 qubits can be generated via our nonadiabatic control theory with 3 steps. In particular, we consider the first and third qubits are longitudinally coupled to the second one with the same coupling strength  $J$  and each qubit is driven by a local laser field. The full Hamiltonian reads

$$H(t) = H + H_d(t) \quad (41)$$

with

$$\begin{aligned} H &= \frac{\omega}{2}(\sigma_1^z + \sigma_2^z + \sigma_3^z) + \frac{J}{2}(\sigma_1^z \sigma_2^z + \sigma_2^z \sigma_3^z), \\ H_d(t) &= e^{i\omega_0 t} [\Omega_0(t) e^{i\varphi_0(t)} |e\rangle_1 \langle g| \\ &\quad + \Omega_1(t) e^{i\varphi_1(t)} |e\rangle_2 \langle g| + \Omega_2(t) e^{i\varphi_2(t)} |e\rangle_3 \langle g|] + \text{H.c.}, \end{aligned} \quad (42)$$

where  $\Omega_n(t)$  is the Rabi-frequency,  $\omega_0$  is the common driving frequency, and  $\varphi_n(t)$  is the driving phase. In the rotating frame with respect to  $H$  (42), the full Hamiltonian (41) is rewritten as

$$\begin{aligned} H_{\text{rot}}(t) &= e^{i(\omega + \omega_0 - J)t} [\Omega_0(t) e^{i\varphi_0(t)} (e^{i2Jt} |ee\rangle_{12} \langle ge| \\ &\quad + |eg\rangle_{12} \langle gg|) \otimes \mathcal{I}_3 + \Omega_1(t) e^{i(Jt + \varphi_1(t))} (e^{i2Jt} |eee\rangle \langle ege| \\ &\quad + |eeg\rangle \langle egg| + |gee\rangle \langle gge| + e^{-i2Jt} |geg\rangle \langle ggg|) \\ &\quad + \Omega_2(t) e^{i\varphi_2(t)} \mathcal{I}_1 \otimes (e^{i2Jt} |ee\rangle_{23} \langle eg| + |ge\rangle_{23} \langle gg|)] + \text{H.c.}, \end{aligned} \quad (43)$$

where  $\mathcal{I}_n$  denotes the identity operator of the  $n$ th qubit.

*Step 1*— Similar to the first step in Sec. III A, this step contributes to pushing the system from the ground state  $|ggg\rangle$  to the first intermediate state  $(|eg\rangle + |ge\rangle)/\sqrt{2} \otimes |g\rangle$ , during which the driving field on the 3rd qubit and the coupling between the 2nd and 3rd qubits are switched off, i.e.,  $\Omega_2(t) = 0$ . Under the driving frequency  $\omega_0 = -\omega + J$  and the strong coupling strength  $J \gg \Omega_0(t), \Omega_1(t)$ , the Hamiltonian  $H_{\text{rot}}(t)$  (43) can be effectively written as

$$\begin{aligned} H_{\text{eff}}^{(1)} &= \Omega_0(t) e^{i\varphi_0} (|ege\rangle \langle gge| + |egg\rangle \langle ggg|) \\ &\quad + \Omega_1(t) e^{i\varphi_1} (|gee\rangle \langle gge| + |geg\rangle \langle ggg|) + \text{H.c.} \end{aligned} \quad (44)$$

under the rotating-wave approximation. As shown in Fig. 6(a), the transitions  $|eee\rangle \leftrightarrow |ege\rangle$ ,  $|eee\rangle \leftrightarrow |gee\rangle$ ,  $|eeg\rangle \leftrightarrow |egg\rangle$ , and  $|eeg\rangle \leftrightarrow |geg\rangle$  indicated by the gray



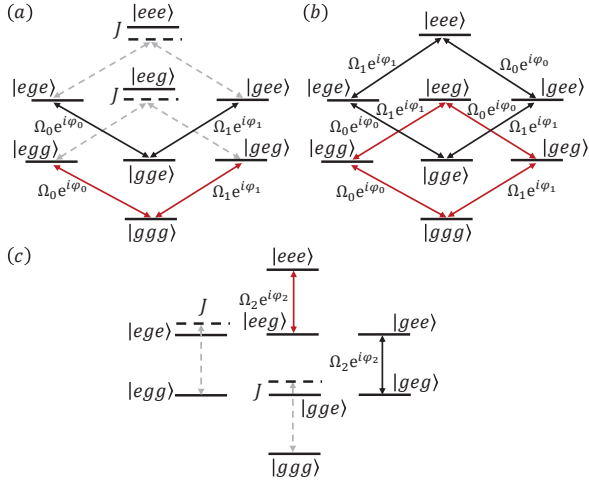


FIG. 6. Step-wise transition diagrams for the longitudinally coupled three-qubit system for (a) the interaction between the 2nd qubit and the 3rd qubit is turned off, the Rabi frequency  $\Omega_2(t) = 0$ , the driving frequency  $\omega_0 = -\omega + J$ , and  $J \gg \Omega_0(t), \Omega_1(t)$ ; (b) when  $\Omega_2(t) = 0$ ,  $\omega_0 = -\omega$ , and  $J = 0$ ; and (c) when the interaction between the 1st qubit and the 2nd qubit is turned off,  $\Omega_0(t) = 0$ ,  $\Omega_1(t) = 0$ ,  $\omega_0 = -\omega - J$ , and  $J \gg \Omega_2(t)$ . The transitions indicated by the gray dashed lines are suppressed due to the strong longitudinal interaction, and the transitions evolving the generation of GHZ state are distinguished by the red solid lines.

dashed lines are suppressed due to the strong longitudinal interaction. The states  $|ggg\rangle$ ,  $|egg\rangle$ , and  $|geg\rangle$  then constitute a 1 + 2-dimensional subspace, which has been illustrated in Sec. II C or Sec. III A. Similar to Eqs. (33) and (34) for the two-qubit system, the ancillary bases in this step can be written as

$$\begin{aligned} |\mu_0(t)\rangle &= \cos \theta_0(t)|egg\rangle - \sin \theta_0(t)e^{-i\alpha_0(t)}|geg\rangle, \\ |\mu_1(t)\rangle &= \cos \phi(t)|b_0(t)\rangle - \sin \phi(t)e^{-i\alpha(t)}|ggg\rangle, \\ |\mu_2(t)\rangle &= \sin \phi(t)|b_0(t)\rangle + \cos \phi(t)e^{-i\alpha(t)}|ggg\rangle, \end{aligned} \quad (45)$$

where  $|b_0(t)\rangle = \sin \theta_0(t)|egg\rangle + \cos \theta_0(t)e^{-i\alpha_0(t)}|geg\rangle$ . Under the same conditions as in Eq. (35),  $|\mu_1(t)\rangle$  and  $|\mu_2(t)\rangle$  can be used as the nonadiabatic passages. With no loss of generality, the system can evolve as  $|ggg\rangle \rightarrow \sin \theta_0(t)|egg\rangle + \cos \theta_0(t)e^{-i\alpha_0(t)}|geg\rangle$  via  $|\mu_1(t)\rangle$  under the boundary conditions  $\alpha(t) = \pi$ ,  $\phi(0) = \pi/2$ , and  $\phi(T) = 0$ . If we further set  $\alpha_0(t) = 0$  and  $\theta_0(t) = \pi/4$ , then the system can evolve to  $(|egg\rangle + |geg\rangle)/\sqrt{2}$ .

*Step 2*— Again similar to the second step in Sec. III A, we convert the system from  $(|egg\rangle + |geg\rangle)/\sqrt{2}$  to  $(|eeg\rangle - |ggg\rangle)/\sqrt{2}$  during this step by setting  $J = 0$ . Under the driving frequency  $\omega_0 = -\omega$  on the first two qubits, the Hamiltonian (43) can be written as

$$\begin{aligned} H_{\text{eff}}^{(2)} &= \Omega_0(t)e^{i\varphi_0}(|eee\rangle\langle gee| + |eeg\rangle\langle geg| \\ &\quad + |geg\rangle\langle gge| + |egg\rangle\langle ggg|) \\ &\quad + \Omega_1(t)e^{i\varphi_1}(|eee\rangle\langle ege| + |eeg\rangle\langle eeg| \\ &\quad + |gee\rangle\langle gge| + |geg\rangle\langle ggg|) + \text{H.c.} \end{aligned} \quad (46)$$

In Fig. 6(b), we therefore have double 2 + 2-dimensional subspaces. The first one is  $\{|ggg\rangle, |eeg\rangle, |leg\rangle, |geg\rangle\}$  and the second one is  $\{|gge\rangle, |eee\rangle, |ege\rangle, |gee\rangle\}$ . Since in the end of last step, the system is only populated on  $|egg\rangle$  and  $|geg\rangle$ , we here focus on the first subspace which can be further divided into the assistant subspace spanned by  $|eeg\rangle$  and  $|ggg\rangle$  and the working subspace spanned by  $|egg\rangle$  and  $|geg\rangle$ . Similar to Eq. (37), the ancillary bases can be chosen as

$$\begin{aligned} |\tilde{\mu}_0(t)\rangle &= \sin \tilde{\theta}_0(t)|eeg\rangle + \cos \tilde{\theta}_0(t)e^{-i\tilde{\alpha}_0(t)}|ggg\rangle, \\ |\mu_0(t)\rangle &= \cos \theta_0(t)|egg\rangle - \sin \theta_0(t)e^{-i\alpha_0(t)}|geg\rangle, \\ |\mu_1(t)\rangle &= \cos \phi(t)|b_0(t)\rangle - \sin \phi(t)e^{-i\alpha(t)}|\tilde{b}_0(t)\rangle, \\ |\mu_2(t)\rangle &= \sin \phi(t)|b_0(t)\rangle + \cos \phi(t)e^{-i\alpha(t)}|\tilde{b}_0(t)\rangle, \end{aligned} \quad (47)$$

where the bright states are

$$\begin{aligned} |\tilde{b}_0(t)\rangle &= \cos \tilde{\theta}_0(t)|eeg\rangle - \sin \tilde{\theta}_0(t)e^{-i\tilde{\alpha}_0(t)}|ggg\rangle, \\ |b_0(t)\rangle &= \sin \theta_0(t)|egg\rangle + \cos \theta_0(t)e^{-i\alpha_0(t)}|geg\rangle. \end{aligned} \quad (48)$$

Under the conditions in Eq. (39) with  $\alpha_0(t) = 0$ ,  $\tilde{\alpha}_0(t) = 0$ ,  $\alpha(t) = \pi$ ,  $\phi(T) = 0$ , and  $\phi(2T) = \pi/2$ , the states can be converted from the state  $(|egg\rangle + |geg\rangle)/\sqrt{2}$  to the state  $(|eeg\rangle - |ggg\rangle)/\sqrt{2}$  via  $|\mu_1(t)\rangle$ .

*Step 3*— In this step, we can evolve the system from the intermediated state  $(|eeg\rangle - |ggg\rangle)/\sqrt{2}$  to the GHZ state  $(|eee\rangle - |ggg\rangle)/\sqrt{2}$  by turning off the coupling between the 1st and 2nd qubits and the driving fields on them, i.e.,  $\Omega_0(t) = 0$  and  $\Omega_1(t) = 0$ . Turning on the driving on the 3rd qubit with the driving frequency  $\omega_0 = -\omega - J$  with  $J \gg \Omega_2(t)$  between the 2nd and 3rd qubits, the Hamiltonian in Eq. (43) reduces to

$$H_{\text{eff}}^{(3)} = \Omega_2(t)e^{i\varphi_2(t)}(|eee\rangle\langle eeg| + |gee\rangle\langle geg|) + \text{H.c.} \quad (49)$$

under the rotating-wave approximation. The associated transition diagram is shown in Fig. 6(c). It is found that transition  $|ggg\rangle \leftrightarrow |gge\rangle$  is averaged out in the system dynamics due to the strong longitudinal interaction. A previous protocol about the generation of a three-qubit GHZ state in a superconducting circuit system [18] is based on the ultrastrong longitudinal interaction between the qubits. It demands  $J \sim \omega$  and then is challenge in experiment. In contrast, we take advantage of a tunable driving frequency  $\omega_0$  to avoid the requirement about the coupling strength.

We here focus on the subspace spanned by  $|eeg\rangle$  and  $|eee\rangle$ . The two ancillary bases can be chosen as

$$\begin{aligned} |\mu_0(t)\rangle &= \cos \phi(t)|eeg\rangle - \sin \phi(t)e^{-i\alpha(t)}|eee\rangle, \\ |\mu_1(t)\rangle &= \sin \phi(t)|eeg\rangle + \cos \phi(t)e^{-i\alpha(t)}|eee\rangle. \end{aligned} \quad (50)$$

Substituting them into the von Neumann equation (5) with the Hamiltonian in Eq. (49), we have the phase and the Rabi frequency as

$$\begin{aligned} \Omega_2(t) &= -\frac{\dot{\phi}(t)}{\sin[\varphi_2(t) + \alpha(t)]}, \\ \dot{\alpha}(t) &= -2\dot{\phi}(t) \cot[\varphi_2(t) + \alpha(t)] \cot 2\phi(t). \end{aligned} \quad (51)$$

Under the conditions in Eq. (51) with  $\alpha(t) = \pi$ ,  $\phi(2T) = 0$ , and  $\phi(3T) = \pi/2$ , the system can be transferred to the GHZ state  $(|eee\rangle - |ggg\rangle)/\sqrt{2}$  via  $|\mu_0(t)\rangle$ .

Similar to Eq. (40), the three-qubit system dynamics  $\rho(t)$  in presence of the dissipation noise can be calculated by the master equation

$$\frac{\partial \rho}{\partial t} = -i[H(t), \rho] + \frac{\kappa}{2}\mathcal{L}(\sigma_1^-) + \frac{\kappa}{2}\mathcal{L}(\sigma_2^-) + \frac{\kappa}{2}\mathcal{L}(\sigma_3^-), \quad (52)$$

where  $H(t)$  is the full Hamiltonian (41) and the dissipation rates for the three qubits are set as the same value  $\kappa$  for simplicity.

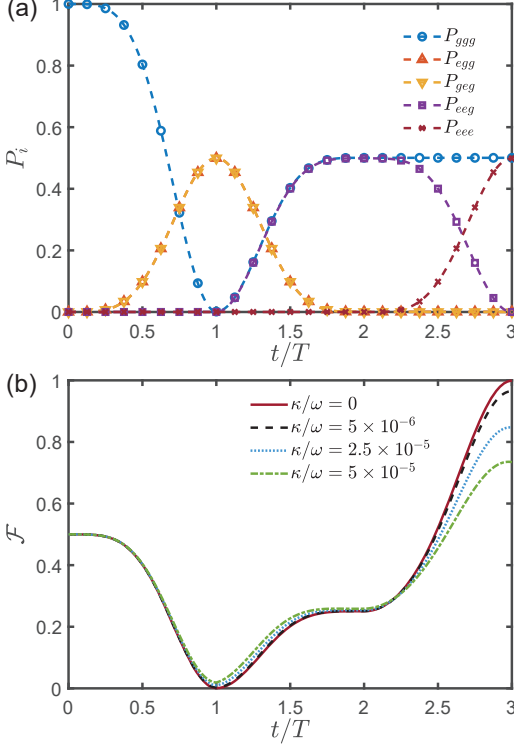


FIG. 7. (a): Populations dynamics for the closed system, and (b) Target-state fidelity dynamics about the 3-qubit GHZ state. When  $t \in [0, 2T]$ , the parameters are set the same as those in Fig. 5; and when  $t \in [2T, 3T]$ ,  $\alpha(t) = \pi$ ,  $\varphi(t) = \pi/2$ ,  $\phi(t) = -(\pi/2) \cos[\pi t/(2T)]$ , and the Rabi frequency  $\Omega_2(t)$  and the phase  $\varphi_2(t)$  are set as Eq. (51).

The dynamics about the level populations  $P_n$  ( $n = ggg, egg, geg, eeg, eee$  for all the involved levels in the above three steps) and the target-state fidelity  $F = \langle \psi_{\text{GHZ}} | \rho(t) | \psi_{\text{GHZ}} \rangle$  with  $|\psi_{\text{GHZ}}\rangle = (|eee\rangle - |ggg\rangle)/\sqrt{2}$  are demonstrated in Figs. 7(a) and (b), respectively. During the first step  $t \in [0, T]$  as shown in Fig. 7(a), the population on the ground state  $|ggg\rangle$  are equally transferred to the levels  $|egg\rangle$  and  $|geg\rangle$ . The other states are not populated during this process. During the second step  $t \in [T, 2T]$ , the populations on the states  $|egg\rangle$  and  $|geg\rangle$  can be synchronically converted to the states  $|ggg\rangle$  and  $|eeg\rangle$  until they are equally populated as  $P_{ggg} = P_{eeg} = 0.5$ . Then during the third step

$t \in [2T, 3T]$ , the population on the state  $|eeg\rangle$  can be fully transferred to the state  $|eee\rangle$  and that on the state  $|ggg\rangle$  remains invariant due to the fact that  $|ggg\rangle$  is decoupled from the system dynamics indicated by Fig. 6(c). Figure 7(b) shows the decoherence effect on the state fidelity. In the end of the control with  $t = 3T$ , one can have a faithful GHZ state  $(|eee\rangle - |ggg\rangle)/\sqrt{2}$  in the absence of dissipation  $\kappa/\omega = 0$ . The fidelity decreases with increasing  $\kappa$ . It is over  $F = 0.965$  when  $\kappa/\omega = 5 \times 10^{-6}$  and reduces to  $F = 0.735$  when  $\kappa/\omega = 5 \times 10^{-5}$ .

### C. N-qubit system

We can generate the  $N$ -qubit GHZ state on a generalized Hamiltonian of that in Eq. (41) within  $N$  steps. In particular, we require that the  $n$ th qubit ( $1 \leq n \leq N-1$ ) is longitudinally interacted with the  $(n+1)$ th one with the same coupling strength  $J$ , and each qubit is driven by a local laser field of the same frequency. The full Hamiltonian can therefore be written as

$$H(t) = H_0 + H_I + H_d(t), \quad (53)$$

where

$$\begin{aligned} H_0 &= \frac{\omega}{2} \sum_{n=1}^N \sigma_n^z, \\ H_I &= \frac{J}{2} \sum_{n=1}^{N-1} \sigma_n^z \sigma_{n+1}^z, \\ H_d(t) &= \sum_{n=1}^N \Omega_n(t) e^{i[\omega_0 t + \varphi_n(t)]} |e\rangle_n \langle g| + \text{H.c.}, \end{aligned} \quad (54)$$

where  $\Omega_n(t)$  is the Rabi frequency,  $\omega_0(t)$  is the common driving frequency of  $N$  laser fields, and  $\varphi_n(t)$  is the time-dependent phase. In the rotating frame with respect to  $H_0$ , the Hamiltonian  $H(t)$  (53) can be transformed to be

$$H_{\text{int}}(t) = H_I + \sum_{n=1}^N \Omega_n(t) e^{i[(\omega + \omega_0)t + \varphi_n]} |e\rangle_n \langle g| + \text{H.c.} \quad (55)$$

*Step 1*— Similar to the first step in Sec. III A or Sec. III B, this step targets to prepare the system to be the intermediate state  $(|eg\rangle + |ge\rangle)/\sqrt{2} \otimes |g\rangle^{\otimes(N-2)}$  from the ground state  $|g\rangle^{\otimes N}$ . We turn on merely the driving fields on the first two qubits and their coupling and set  $\omega_0 = -\omega + J$  with  $J \gg \{\Omega_0, \Omega_1\}$ . The rotating Hamiltonian with respect to  $H_I$  can then be expressed as

$$\begin{aligned} H_{\text{eff}}^{(1)} &= \Omega_0(t) e^{i\varphi_0(t)} |eg \cdots gg\rangle \langle gg \cdots gg| \\ &+ \Omega_1(t) e^{i\varphi_1(t)} |ge \cdots gg\rangle \langle gg \cdots gg| + \text{H.c.} \end{aligned} \quad (56)$$

under the rotating-wave approximation. Here the states  $|gg\rangle \otimes |g\rangle^{\otimes(N-2)}$ ,  $|ge\rangle \otimes |g\rangle^{\otimes(N-2)}$ , and  $|eg\rangle \otimes |g\rangle^{\otimes(N-2)}$  constitute a  $1 + 2$ -dimensional subspace. The ancillary

bases in this step can be obtained by extending Eq. (45) for the 3-qubit system:

$$\begin{aligned} |\mu_0(t)\rangle &= \cos \theta_0(t) |eg \cdots gg\rangle - \sin \theta_0(t) e^{-i\alpha_0(t)} |ge \cdots gg\rangle, \\ |\mu_1(t)\rangle &= \cos \phi(t) |b_0(t)\rangle - \sin \phi(t) e^{-i\alpha(t)} |gg \cdots gg\rangle, \\ |\mu_2(t)\rangle &= \sin \phi(t) |b_0(t)\rangle + \cos \phi(t) e^{-i\alpha(t)} |gg \cdots gg\rangle, \end{aligned} \quad (57)$$

where the bright state is  $|b_0(t)\rangle = \sin \theta_0(t) |eg \cdots gg\rangle + \cos \theta_0(t) e^{-i\alpha_0(t)} |ge \cdots gg\rangle$ . When the driving fields follow Eq. (35) with the boundary conditions  $\alpha_0(t) = 0$ ,  $\alpha(t) = \pi$ ,  $\phi(0) = \pi/2$  and  $\phi(T) = 0$ , the system can evolve from  $|gg\rangle \otimes |g\rangle^{\otimes(N-2)}$  to  $(|eg\rangle + |ge\rangle)/\sqrt{2} \otimes |g\rangle^{\otimes(N-2)}$  via the passage  $|\mu_1(t)\rangle$ .

*Step 2*— Again similar to the second step in Sec. III A or Sec. III B, this step converts the system from  $(|eg\rangle + |ge\rangle)/\sqrt{2} \otimes |g\rangle^{\otimes(N-2)}$  to  $(|ee\rangle - |gg\rangle)/\sqrt{2} \otimes |g\rangle^{\otimes(N-2)}$ . We turn off the longitudinal interaction among the first two qubits and set the driving frequency as  $\omega_0 = -\omega$ . The effective Hamiltonian then becomes

$$\begin{aligned} H_{\text{eff}}^{(2)} &= \Omega_0(t) e^{i\varphi_0(t)} (|eg \cdots gg\rangle \langle gg \cdots gg| \\ &\quad + |ee \cdots gg\rangle \langle ge \cdots gg|) \\ &\quad + \Omega_1(t) e^{i\varphi_1(t)} (|ge \cdots gg\rangle \langle gg \cdots gg| \\ &\quad + |ee \cdots gg\rangle \langle eg \cdots gg|) + \text{H.c.}, \end{aligned} \quad (58)$$

which forms a 2 + 2-dimensional system. The ancillary bases can be written as

$$\begin{aligned} |\tilde{\mu}_0(t)\rangle &= \sin \tilde{\theta}_0(t) |ee \cdots gg\rangle + \cos \tilde{\theta}_0(t) e^{-i\tilde{\alpha}_0(t)} |gg \cdots gg\rangle, \\ |\mu_0(t)\rangle &= \cos \theta_0(t) |eg \cdots gg\rangle - \sin \theta_0(t) e^{-i\alpha_0(t)} |ge \cdots gg\rangle, \\ |\mu_1(t)\rangle &= \cos \phi(t) |b_0(t)\rangle - \sin \phi(t) e^{-i\alpha(t)} |\tilde{b}_0(t)\rangle, \\ |\mu_2(t)\rangle &= \sin \phi(t) |b_0(t)\rangle + \cos \phi(t) e^{-i\alpha(t)} |\tilde{b}_0(t)\rangle, \end{aligned} \quad (59)$$

where the bright states are

$$\begin{aligned} |\tilde{b}_0(t)\rangle &\equiv \cos \tilde{\theta}_0(t) |ee \cdots gg\rangle - \sin \tilde{\theta}_0(t) e^{-i\tilde{\alpha}_0(t)} |gg \cdots gg\rangle, \\ |b_0(t)\rangle &\equiv \sin \theta_0(t) |eg \cdots gg\rangle + \cos \theta_0(t) e^{-i\alpha_0(t)} |ge \cdots gg\rangle. \end{aligned} \quad (60)$$

With the phases and Rabi-frequencies in Eq. (39) and the boundary conditions  $\alpha_0(t) = 0$ ,  $\tilde{\alpha}_0(t) = 0$ ,  $\alpha(t) = \pi$ ,  $\phi(T) = 0$ , and  $\phi(2T) = \pi/2$ , the system can be transferred to be  $(|ee\rangle - |gg\rangle)/\sqrt{2} \otimes |g\rangle^{\otimes(N-2)}$  via the passage  $|\mu_1(t)\rangle$ .

*Step k* ( $3 \leq k \leq N$ )— Similar to the third step in Sec. III B, the  $k$ th step is used to transform the system from the state  $(|e\rangle^{\otimes(k-1)} - |g\rangle^{\otimes(k-1)})/\sqrt{2} \otimes |g\rangle^{\otimes(N-k+1)}$  to the state  $(|e\rangle^{\otimes k} - |g\rangle^{\otimes k})/\sqrt{2} \otimes |g\rangle^{\otimes(N-k)}$ ,  $3 \leq k \leq N$ . In the  $k$ th step, we hold exclusively the longitudinal interaction between the  $(k-1)$ th and  $k$ th qubits and the driving fields on the  $k$ th qubit. With  $\omega_0 = -\omega - J$  and  $J \gg \Omega_k(t)$ , the rotating Hamiltonian with respect to  $H_I$  can then be approximated by

$$\begin{aligned} H_{\text{eff}}^{(k)} &= \Omega_k(t) e^{i\varphi_k(t)} \\ &\quad \times |ee \cdots e_k \cdots gg\rangle \langle ee \cdots g_k \cdots gg| + \text{H.c.}, \end{aligned} \quad (61)$$

Similar to the (1 + 1)-dimensional system in Sec. II C and Sec. III B, the ancillary bases for the nonadiabatic passage can be chosen from

$$\begin{aligned} |\mu_0(t)\rangle^{(k)} &= \cos \phi(t) |ee \cdots e_k \cdots gg\rangle \\ &\quad - \sin \phi(t) e^{-i\alpha(t)} |ee \cdots g_k \cdots gg\rangle, \\ |\mu_1(t)\rangle^{(k)} &= \sin \phi(t) |ee \cdots e_k \cdots gg\rangle \\ &\quad + \cos \phi(t) e^{-i\alpha(t)} |ee \cdots g_k \cdots gg\rangle, \end{aligned} \quad (62)$$

where the superscript  $k$  indicates the  $k$ th step. When the driving fields satisfy the conditions in Eq. (51), the system can evolve from the state  $(|e\rangle^{\otimes(k-1)} - |g\rangle^{\otimes(k-1)})/\sqrt{2} \otimes |g\rangle^{\otimes(N-k+1)}$  to the state  $(|e\rangle^{\otimes k} - |g\rangle^{\otimes k})/\sqrt{2} \otimes |g\rangle^{\otimes(N-k)}$  via the passage  $|\mu_0(t)\rangle^{(k)}$  by setting  $\alpha(t) = \pi$ ,  $\phi[(k-1)T] = \pi/2$ , and  $\phi(kT) = \pi$ . Here  $T$  is the running time for every step. With  $N-2$  iteration of such a controlled evolution, the system will end up with a multi-particle GHZ state as  $(|e\rangle^{\otimes N} - |g\rangle^{\otimes N})/\sqrt{2}$ .

## IV. CONCLUSION

In summary, we develop a full-fledged nonadiabatic control theory for the popular atomic models with two subspaces, e.g., the assistant and working subspaces. We provide a systematic method for constructing the parametric ancillary bases crossing the two subspaces and determine the sufficient conditions for them to be useful nonadiabatic passages. In addition, we find the sufficient conditions to convert the static dark states inside the assistant or working subspace to full-featured state-transfer paths. The general theory is applied to prepare the maximal entangled states of distant systems with a high fidelity. By virtue of the longitudinal interaction between neighboring qubits in a superconducting circuit system, we can generate the Bell states and the  $N$ -qubit GHZ state and realize mutual transfer between the single-excitation Bell state and the double-excitation Bell state. Our work improves the theory framework for nonadiabatic quantum control over discrete systems and is interesting to preparing distant entangled states in a future quantum network.

## ACKNOWLEDGMENTS

We acknowledge grant support from the National Natural Science Foundation of China (Grant No. 11974311).

### Appendix A: A brief recipe of ancillary bases

This appendix contributes to explicitly constructing  $M + N$  ancillary bases in Eqs. (10), (11), and (12) and  $M + N - 2$  bright states in Eq. (13) for our general model described in Fig. 1 or the full Hamiltonian (9). They follow the orthonormal relations as  $\langle \tilde{\mu}_m(t) | \tilde{b}_m(t) \rangle = 0$

and  $\langle \mu_n(t) | b_n(t) \rangle = 0$  with  $0 \leq m \leq M-2$  and  $0 \leq n \leq N-2$  and  $\langle \mu_{N-1}(t) | \mu_N(t) \rangle = 0$ . The construction order is suggested to be (i)  $\{|e_0\rangle, |e_1\rangle\} \rightarrow \{|\tilde{\mu}_0(t)\rangle, |\tilde{b}_0(t)\rangle\}, \{|\tilde{b}_0(t)\rangle, |e_2\rangle\} \rightarrow \{|\tilde{\mu}_1(t)\rangle, |\tilde{b}_1(t)\rangle\}, \dots, \{|\tilde{b}_{M-3}(t)\rangle, |e_{M-1}\rangle\} \rightarrow \{|\tilde{\mu}_{M-2}(t)\rangle, |\tilde{b}_{M-2}(t)\rangle\}$  for the assistant subspace; (ii)  $\{|0\rangle, |1\rangle\} \rightarrow \{|\mu_0(t)\rangle, |b_0(t)\rangle\}, \{|b_0(t)\rangle, |2\rangle\} \rightarrow \{|\mu_1(t)\rangle, |b_1(t)\rangle\}, \dots, \{|b_{N-3}(t)\rangle, |N-1\rangle\} \rightarrow \{|\mu_{N-2}(t)\rangle, |b_{N-2}(t)\rangle\}$  for the working subspace; and eventually (iii)  $\{|\tilde{b}_{M-2}(t)\rangle, |b_{N-2}\rangle\} \rightarrow |\mu_{N-1}(t)\rangle, |\mu_N(t)\rangle$ .

Using a SU(2)-like rotation matrix, the bases  $|\tilde{\mu}_m(t)\rangle$  and  $|\tilde{b}_m(t)\rangle$ ,  $0 \leq m \leq M-2$ , are determined by the preceding sequence (i) as the superposition over the upper bright state and the upper (assistant) levels. They can be formulated as

$$\begin{aligned} & \begin{pmatrix} |\tilde{\mu}_m(t)\rangle \\ |\tilde{b}_m(t)\rangle \end{pmatrix} \\ &= \begin{pmatrix} \sin \tilde{\theta}_m(t) & \cos \tilde{\theta}_m(t) e^{-i\tilde{\alpha}_m(t)} \\ \cos \tilde{\theta}_m(t) & -\sin \tilde{\theta}_m(t) e^{-i\tilde{\alpha}_m(t)} \end{pmatrix} \begin{pmatrix} |\tilde{b}_{m-1}(t)\rangle \\ |e_{m+1}\rangle \end{pmatrix}, \end{aligned} \quad (\text{A1})$$

where  $|\tilde{b}_{-1}(t)\rangle \equiv |e_0\rangle$ . Similarly, the sequence (ii) deter-

mines the bases  $|\mu_n(t)\rangle$  and  $|b_n(t)\rangle$ ,  $0 \leq n \leq N-2$ , as the superposition over the down bright state and the down (working) levels:

$$\begin{aligned} & \begin{pmatrix} |\mu_n(t)\rangle \\ |b_n(t)\rangle \end{pmatrix} \\ &= \begin{pmatrix} \cos \theta_n(t) & -\sin \theta_n(t) e^{-i\alpha_n(t)} \\ \sin \theta_n(t) & \cos \theta_n(t) e^{-i\alpha_n(t)} \end{pmatrix} \begin{pmatrix} |b_{n-1}(t)\rangle \\ |n+1\rangle \end{pmatrix}, \end{aligned} \quad (\text{A2})$$

where  $|b_{-1}(t)\rangle \equiv |0\rangle$ . The rest two ancillary bases  $|\mu_{N-1}(t)\rangle$  and  $|\mu_N(t)\rangle$  are then constructed by the last bright states in the two subspaces:

$$\begin{aligned} & \begin{pmatrix} |\mu_{N-1}(t)\rangle \\ |\mu_N(t)\rangle \end{pmatrix} \\ &= \begin{pmatrix} \cos \phi(t) & -\sin \phi(t) e^{-i\alpha(t)} \\ \sin \phi(t) & \cos \phi(t) e^{-i\alpha(t)} \end{pmatrix} \begin{pmatrix} |b_{N-1}(t)\rangle \\ |\tilde{b}_{M-2}(t)\rangle \end{pmatrix}. \end{aligned} \quad (\text{A3})$$

Finally, we have a completed and orthonormal set of bases to span the whole Hilbert space of our  $M+N$ -dimensional system.

- 
- [1] A. Einstein, B. Podolsky, and N. Rosen, *Can quantum-mechanical description of physical reality be considered complete?* *Phys. Rev.* **47**, 777 (1935).
- [2] N. Bohr, *Can quantum-mechanical description of physical reality be considered complete?* *Phys. Rev.* **48**, 696 (1935).
- [3] R. Horodecki, P. Horodecki, M. Horodecki, and K. Horodecki, *Quantum entanglement*, *Rev. Mod. Phys.* **81**, 865 (2009).
- [4] C. H. Bennett, *Quantum information*, *Phys. Scr.* **1998**, 210 (1998).
- [5] T. D. Ladd, F. Jelezko, R. Laflamme, Y. Nakamura, C. Monroe, and J. L. O'Brien, *Quantum computers*, *Nature* **464**, 45 (2010).
- [6] I. Buluta, S. Ashhab, and F. Nori, *Natural and artificial atoms for quantum computation*, *Rep. Prog. Phys.* **74**, 104401 (2011).
- [7] H. J. Kimble, *The quantum internet*, *Nature* **453**, 1023 (2008).
- [8] N. Gisin and R. Thew, *Quantum communication*, *Nat. Photon.* **1**, 165 (2007).
- [9] G. Wendin, *Quantum information processing with superconducting circuits: a review*, *Rep. Prog. Phys.* **80**, 106001 (2017).
- [10] C. H. Bennett, G. Brassard, C. Crépau, R. Jozsa, A. Peres, and W. K. Wootters, *Teleporting an unknown quantum state via dual classical and einstein-podolsky-rosen channels*, *Phys. Rev. Lett.* **70**, 1895 (1993).
- [11] A. K. Ekert, *Quantum cryptography based on bell's theorem*, *Phys. Rev. Lett.* **67**, 661 (1991).
- [12] G. L. Long and X. S. Liu, *Theoretically efficient high-capacity quantum-key-distribution scheme*, *Phys. Rev. A* **65**, 032302 (2002).
- [13] M. Hillery, V. Bužek, and A. Berthiaume, *Quantum secret sharing*, *Phys. Rev. A* **59**, 1829 (1999).
- [14] F.-G. Deng, G. L. Long, and X.-S. Liu, *Two-step quantum direct communication protocol using the einstein-podolsky-rosen pair block*, *Phys. Rev. A* **68**, 042317 (2003).
- [15] H.-J. Briegel, W. Dür, J. I. Cirac, and P. Zoller, *Quantum repeaters: The role of imperfect local operations in quantum communication*, *Phys. Rev. Lett.* **81**, 5932 (1998).
- [16] N. Brunner, D. Cavalcanti, S. Pironio, V. Scarani, and S. Wehner, *Bell nonlocality*, *Rev. Mod. Phys.* **86**, 419 (2014).
- [17] D. Bouwmeester, J.-W. Pan, M. Daniell, H. Weinfurter, and A. Zeilinger, *Observation of three-photon greenberger-horne-zeilinger entanglement*, *Phys. Rev. Lett.* **82**, 1345 (1999).
- [18] L. F. Wei, Y.-x. Liu, and F. Nori, *Generation and control of greenberger-horne-zeilinger entanglement in superconducting circuits*, *Phys. Rev. Lett.* **96**, 246803 (2006).
- [19] W. Dür, G. Vidal, and J. I. Cirac, *Three qubits can be entangled in two inequivalent ways*, *Phys. Rev. A* **62**, 062314 (2000).
- [20] J. Lee and M. S. Kim, *Entanglement teleportation via werner states*, *Phys. Rev. Lett.* **84**, 4236 (2000).
- [21] J. J. Bollinger, W. M. Itano, D. J. Wineland, and D. J. Heinzen, *Optimal frequency measurements with maximally correlated states*, *Phys. Rev. A* **54**, R4649 (1996).
- [22] V. Giovannetti, S. Lloyd, and L. Maccone, *Quantum-enhanced measurements: Beating the standard quantum limit*, *Science* **306**, 1330 (2004).
- [23] S.-B. Zheng, *One-step synthesis of multiatom greenberger-horne-zeilinger states*, *Phys. Rev. Lett.* **87**, 230404 (2001).
- [24] G.-P. Guo, C.-F. Li, J. Li, and G.-C. Guo, *Scheme for*

- the preparation of multiparticle entanglement in cavity qed, *Phys. Rev. A* **65**, 042102 (2002).
- [25] H. Y. Yuan, P. Yan, S. Zheng, Q. Y. He, K. Xia, and M.-H. Yung, *Steady bell state generation via magnon-photon coupling*, *Phys. Rev. Lett.* **124**, 053602 (2020).
- [26] S.-f. Qi and J. Jing, *Generation of bell and greenberger-horne-zeilinger states from a hybrid qubit-photon-magnon system*, *Phys. Rev. A* **105**, 022624 (2022).
- [27] V. M. Stojanović, *Bare-excitation ground state of a spinless-fermion-boson model and  $w$ -state engineering in an array of superconducting qubits and resonators*, *Phys. Rev. Lett.* **124**, 190504 (2020).
- [28] W. Feng, G.-Q. Zhang, Q.-P. Su, J.-X. Zhang, and C.-P. Yang, *Generation of greenberger-horne-zeilinger states on two-dimensional superconducting-qubit lattices via parallel multiqubit-gate operations*, *Phys. Rev. Appl.* **18**, 064036 (2022).
- [29] V. M. Stojanović, *Scalable  $w$ -type entanglement resource in neutral-atom arrays with rydberg-dressed resonant dipole-dipole interaction*, *Phys. Rev. A* **103**, 022410 (2021).
- [30] G. Ribordy, J. Brendel, J.-D. Gautier, N. Gisin, and H. Zbinden, *Long-distance entanglement-based quantum key distribution*, *Phys. Rev. A* **63**, 012309 (2000).
- [31] X.-M. Hu, C.-X. Huang, Y.-B. Sheng, L. Zhou, B.-H. Liu, Y. Guo, C. Zhang, W.-B. Xing, Y.-F. Huang, C.-F. Li, and G.-C. Guo, *Long-distance entanglement purification for quantum communication*, *Phys. Rev. Lett.* **126**, 010503 (2021).
- [32] J. Zou, S. Zhang, and Y. Tserkovnyak, *Bell-state generation for spin qubits via dissipative coupling*, *Phys. Rev. B* **106**, L180406 (2022).
- [33] G.-Q. Zhang, W. Feng, W. Xiong, D. Xu, Q.-P. Su, and C.-P. Yang, *Generating bell states and  $n$ -partite  $w$  states of long-distance qubits in superconducting waveguide qed*, *Phys. Rev. Appl.* **20**, 044014 (2023).
- [34] M. Hays, V. Fatemi, D. Bouman, J. Cerrillo, S. Diamond, K. Serniak, T. Connolly, P. Krogstrup, J. Nygård, A. L. Yeyati, A. Geresdi, and M. H. Devoret, *Coherent manipulation of an andreev spin qubit*, *Science* **373**, 430 (2021).
- [35] M. Pita-Vidal, A. Bargerbos, R. Žitko, L. J. Splitthoff, L. Grünhaupt, J. J. Wesdorp, Y. Liu, L. P. Kouwenhoven, R. Aguado, B. van Heck, A. Kou, and C. K. Andersen, *Direct manipulation of a superconducting spin qubit strongly coupled to a transmon qubit*, *Nat. Phys.* **19**, 1110 (2023).
- [36] L. Tosi, C. Metzger, M. F. Goffman, C. Urbina, H. Pothier, S. Park, A. L. Yeyati, J. Nygård, and P. Krogstrup, *Spin-orbit splitting of andreev states revealed by microwave spectroscopy*, *Phys. Rev. X* **9**, 011010 (2019).
- [37] M. Hays, V. Fatemi, K. Serniak, D. Bouman, S. Diamond, G. de Lange, P. Krogstrup, J. Nygård, A. Geresdi, and M. H. Devoret, *Continuous monitoring of a trapped superconducting spin*, *Nat. Phys.* **16**, 1103 (2020).
- [38] J. J. Wesdorp, L. Grünhaupt, A. Vaartjes, M. Pita-Vidal, A. Bargerbos, L. J. Splitthoff, P. Krogstrup, B. van Heck, and G. de Lange, *Dynamical polarization of the fermion parity in a nanowire josephson junction*, *Phys. Rev. Lett.* **131**, 117001 (2023).
- [39] J. J. Wesdorp, F. J. Matute-Cañadas, A. Vaartjes, L. Grünhaupt, T. Laeven, S. Roelofs, L. J. Splitthoff, M. Pita-Vidal, A. Bargerbos, D. J. van Woerkerkom, P. Krogstrup, L. P. Kouwenhoven, C. K. Andersen, A. L. Yeyati, B. van Heck, and G. de Lange, *Microwave spectroscopy of interacting andreev spins*, *Phys. Rev. B* **109**, 045302 (2024).
- [40] A. Bargerbos, M. Pita-Vidal, R. Žitko, L. J. Splitthoff, L. Grünhaupt, J. J. Wesdorp, Y. Liu, L. P. Kouwenhoven, R. Aguado, C. K. Andersen, A. Kou, and B. van Heck, *Spectroscopy of spin-split andreev levels in a quantum dot with superconducting leads*, *Phys. Rev. Lett.* **131**, 097001 (2023).
- [41] M. Pita-Vidal, J. J. Wesdorp, L. J. Splitthoff, A. Bargerbos, Y. Liu, L. P. Kouwenhoven, and C. K. Andersen, *Strong tunable coupling between two distant superconducting spin qubits*, *Nat. Phys.* **20**, 1158 (2024).
- [42] D. Loss and D. P. DiVincenzo, *Quantum computation with quantum dots*, *Phys. Rev. A* **57**, 120 (1998).
- [43] R. Hanson, L. P. Kouwenhoven, J. R. Petta, S. Tarucha, and L. M. K. Vandersypen, *Spins in few-electron quantum dots*, *Rev. Mod. Phys.* **79**, 1217 (2007).
- [44] G. Burkard, T. D. Ladd, A. Pan, J. M. Nichol, and J. R. Petta, *Semiconductor spin qubits*, *Rev. Mod. Phys.* **95**, 025003 (2023).
- [45] N. V. Vitanov, A. A. Rangelov, B. W. Shore, and K. Bergmann, *Stimulated raman adiabatic passage in physics, chemistry, and beyond*, *Rev. Mod. Phys.* **89**, 015006 (2017).
- [46] D. Guéry-Odelin, A. Ruschhaupt, A. Kiely, E. Torrontegui, S. Martínez-Garaot, and J. G. Muga, *Shortcuts to adiabaticity: Concepts, methods, and applications*, *Rev. Mod. Phys.* **91**, 045001 (2019).
- [47] J. Jing, M. S. Sarandy, D. A. Lidar, D.-W. Luo, and L.-A. Wu, *Eigenstate tracking in open quantum systems*, *Phys. Rev. A* **94**, 042131 (2016).
- [48] C. Marr, A. Beige, and G. Rempe, *Entangled-state preparation via dissipation-assisted adiabatic passages*, *Phys. Rev. A* **68**, 033817 (2003).
- [49] L.-B. Chen, M.-Y. Ye, G.-W. Lin, Q.-H. Du, and X.-M. Lin, *Generation of entanglement via adiabatic passage*, *Phys. Rev. A* **76**, 062304 (2007).
- [50] E. Sjöqvist, D. M. Tong, L. M. Andersson, B. Hessmo, M. Johansson, and K. Singh, *Non-adiabatic holonomic quantum computation*, *New J. Phys.* **14**, 103035 (2012).
- [51] B.-J. Liu, X.-K. Song, Z.-Y. Xue, X. Wang, and M.-H. Yung, *Plug-and-play approach to nonadiabatic geometric quantum gates*, *Phys. Rev. Lett.* **123**, 100501 (2019).
- [52] F. Setiawan, P. Groszkowski, H. Ribeiro, and A. A. Clerk, *Analytic design of accelerated adiabatic gates in realistic qubits: General theory and applications to superconducting circuits*, *PRX Quantum* **2**, 030306 (2021).
- [53] X. Chen, I. Lizuain, A. Ruschhaupt, D. Guéry-Odelin, and J. G. Muga, *Shortcut to adiabatic passage in two- and three-level atoms*, *Phys. Rev. Lett.* **105**, 123003 (2010).
- [54] A. Baksic, H. Ribeiro, and A. A. Clerk, *Speeding up adiabatic quantum state transfer by using dressed states*, *Phys. Rev. Lett.* **116**, 230503 (2016).
- [55] Y.-C. Li and X. Chen, *Shortcut to adiabatic population transfer in quantum three-level systems: Effective two-level problems and feasible counterdiabatic driving*, *Phys. Rev. A* **94**, 063411 (2016).
- [56] X. Chen, A. Ruschhaupt, S. Schmidt, A. del Campo, D. Guéry-Odelin, and J. G. Muga, *Fast optimal frictionless atom cooling in harmonic traps: Shortcut to adiabaticity*, *Phys. Rev. Lett.* **104**, 063002 (2010).
- [57] X. Chen, E. Torrontegui, and J. G. Muga, *Lewis-riesenfeld invariants and transitionless quantum driving*,

- Phys. Rev. A* **83**, 062116 (2011).
- [58] S.-f. Qi and J. Jing, *Accelerated adiabatic passage in cavity magnomechanics*, *Phys. Rev. A* **105**, 053710 (2022).
- [59] S. An, D. Lv, A. del Campo, and K. Kim, *Shortcuts to adiabaticity by counterdiabatic driving for trapped-ion displacement in phase space*, *Nat. Commun.* **7**, 12999 (2016).
- [60] Z.-y. Jin and J. Jing, *Shortcut to adiabaticity and holonomic transformation are the same thing*, *arXiv: 2406.16016* (2024).
- [61] J. A. Jones, V. Vedral, A. Ekert, and G. Castagnoli, *Geometric quantum computation using nuclear magnetic resonance*, *Nature* **403**, 869 (2000).
- [62] L.-M. Duan, J. I. Cirac, and P. Zoller, *Geometric manipulation of trapped ions for quantum computation*, *Science* **292**, 1695 (2001).
- [63] J. R. Morris and B. W. Shore, *Reduction of degenerate two-level excitation to independent two-state systems*, *Phys. Rev. A* **27**, 906 (1983).
- [64] H. Carmichael, *Statistical Methods in Quantum Optics* (Springer, Berlin, 1999).
- [65] M. O. Scully and M. S. Zubairy, *Quantum Optics* (Cambridge University Press, Cambridge, 1997).